Relativistic quasiparticle time blocking approximation: Dipole response of open-shell nuclei

E. Litvinova
Gesellschaft für Schwerionenforschung mbH, Planckstraße 1, D-64291 Darmstadt, Germany and
Institute of Physics and Power Engineering, RU-249033 Obninsk, Russia

P. Ring
Physik-Department der Technischen Universität München, D-85748 Garching, Germany and
Departamento de Física Teórica, Universidad Autónoma de Madrid, E-28049 Madrid, Spain

V. Tselyaev
Nuclear Physics Department, V. A. Fock Institute of Physics, St. Petersburg State University, RU-198504 St. Petersburg, Russia
(Received 20 February 2008; revised manuscript received 3 June 2008; published 22 July 2008)

The self-consistent relativistic quasiparticle random-phase approximation (RQRPA) is extended by the quasiparticle-phonon coupling (QPC) model using the quasiparticle time blocking approximation (QTBA). The method is formulated in terms of the Bethe-Salpeter equation (BSE) in the two-quasiparticle space with an energy-dependent two-quasiparticle residual interaction. This equation is solved either in the basis of Dirac states forming the self-consistent solution of the ground state or in the momentum representation. Pairing correlations are treated within the Bardeen-Cooper-Schrieffer (BCS) model with a monopole-monopole interaction. The same NL3 set of the coupling constants generates the Dirac-Hartree-BCS single-quasiparticle spectrum, the static part of the residual two-quasiparticle interaction and the quasiparticle-phonon coupling amplitudes. A quantitative description of electric dipole excitations in the chain of tin isotopes ($Z = 50$) with the mass numbers $A = 100$, 106, 114, 116, 120, and 130 and in the chain of isotones with ($N = 50$) ^{88}Sr, ^{90}Zr, ^{92}Mo is performed within this framework. The RQRPA extended by the coupling to collective vibrations generates spectra with a multitude of $2q \otimes$ phonon (two quasiparticles plus phonon) states providing a noticeable fragmentation of the giant dipole resonance as well as of the soft dipole mode (pygmy resonance) in the nuclei under investigation. The results obtained for the photo absorption cross sections and for the integrated contributions of the low-lying strength to the calculated dipole spectra agree very well with the available experimental data.

DOI: 10.1103/PhysRevC.78.014312 PACS number(s): 21.30.Fe, 21.60.Jz, 24.10.Cn, 27.60.+j

I. INTRODUCTION

Theoretical approaches based on covariant density functional theory (CDFT) remain undoubtedly among the most successful microscopic descriptions of nuclear structure. The CDFT approaches are derived from a Lorentz invariant density functional that connects in a consistent way the spin and spatial degrees of freedom in the nucleus. Therefore, it needs only a relatively small number of parameters that are adjusted to reproduce a set of bulk properties of spherical closed-shell nuclei [1,2] and it is valid over the entire periodic table. Over the years, relativistic mean-field (RMF) models based on the CDFT have been successfully applied to describe ground-state properties of finite spherical and deformed nuclei over the entire nuclear chart [3] from light nuclei [4] to super-heavy elements [5,6] and from the neutron drip line where halo phenomena are observed [7] to the proton drip line [8] with nuclei unstable against the emission of protons [9]. The relativistic cranking approximation has been developed to calculate rotational bands [10,11]. For a description of nuclear excited states, the relativistic random-phase approximation (RRPA) [12] and the quasiparticle RRPA (RQRPA) [13] have been formulated as the small amplitude limit of the time-dependent RMF models. These models have provided a very good description for the positions of giant resonances and a theoretical interpretation of the low-lying dipole [13] and quadrupole [14,15] excitations. Proton-neutron versions of the RRPA and the RQRPA have been developed and successfully applied to the description of spin/isospin excitations as the isobaric analog resonance (IAR) or the Gamow-Teller Resonance (GTR) [16].

Recently, several attempts have been made to extend the RMF and RRPA formalism beyond the mean-field approach, first, to solve the well-known problem of the RMF single-particle level density in the vicinity of the Fermi surface that is too low because of the too-small effective mass. The energy dependence of the single-nucleon self-energy was emulated in a phenomenological way [17] and microscopically by coupling the single-particle configurations to low-lying surface vibration [18]. This provided a considerable improvement for the description of the single-particle spectra. In addition, the quadrupole motion has been studied within the relativistic generator coordinate method (GCM) [19,20].

In Refs. [21,22], we have extended the relativistic RPA by introducing a coupling to collective vibrations using the techniques developed and realized long ago for nonrelativistic approaches in terms of the Green's function formalism [23–26]. An induced additional interaction between single-particle and vibrational excitations provided a strong fragmentation of the pure RRPA states causing the spreading width of giant resonances and the redistribution of the pygmy strength to lower energies. This method does not include

pairing correlations and therefore it is restricted essentially to the few nuclei with doubly closed shells in the nuclear chart.

In the present work we consider systems with pairing correlations. Again, we are guided by ideas of the quasiparticle time-blocking approximation (QTBA) developed and applied for nonrelativistic systems in Refs. [27] and [28], which takes into account quasiparticle-phonon coupling (QPC) and pairing correlations on an equal footing. However, our approach is based on CDFT and formulated in terms of relativistic Green's functions of the Dirac-Hartree-Bardeen-Cooper-Schrieffer (DHBCS) equations. Similar, but in details different, approaches developed earlier within a nonrelativistic formalism can be found in Refs. [29–31].

The main assumption of the quasiparticle-phonon coupling model [32] is that the two types of elementary excitations—two-quasiparticle and vibrational modes—are coupled in such a way that configurations of $2q \otimes$ phonon type with low-lying phonons strongly compete with simple $2q$ configurations close in energy or, in other words, that quasiparticles can emit and absorb phonons with rather high probabilities. Obviously, these processes should affect both the ground and excited states and therefore, the corresponding amplitudes should be taken into account both in the single-nucleon self-energy and in the effective interaction in the nuclear interior.

To describe excited states in nuclei, we extend covariant density functional theory by coupling the quasiparticles to low-lying vibrations in a consistent way using effective interactions derived from the same Lagrangian without additional phenomenological parameters. First of all, we use the well-known quasiparticle formalism, where, in terms of second quantization, nucleon creation and annihilation operators become components of a two-component operator mixing a creation and annihilation of a particle into a single quasiparticle. This leads to the fact that for systems with pairing correlations all quantum operators become tensors in the two-dimensional quasiparticle space. In particular, the relativistic energy functional is expressed in terms of the relativistic extension of the Valatin density matrix [33] of double dimension containing the normal as well as the abnormal densities. As discussed in detail in Refs. [34–37] pairing correlations can be considered in a very good approximation as a non-relativistic effect and therefore the full density functional is a sum of the relativistic energy functional depending on the normal density and derived from the underlying Lagrangian and a nonrelativistic pairing energy E_{pair}, depending on the abnormal density. The equations of motion are the self-consistent relativistic Hartree-Bogoliubov (RHB) equations. They are derived from this general functional by variation with respect to the Valatin density matrix. They are solved numerically and the self-consistent fields obtained in this way, which do not depend on the energy, form the static part of the nucleon self-energy. This static part determines the nuclear ground state in the mean-field approximation.

The static effective interaction used in conventional QRPA approximation is derived as the second derivative of the same energy functional and therefore it contains no additional parameters. It enables us to go a step further and to compute amplitudes, or vertices, that describe the emission or absorption of phonons by quasiparticles within the relativistic framework. These amplitudes form the essential ingredient for the following considerations. They determine an additive energy-dependent and nonlocal term in the self-energy of the single-quasiparticle equation of motion and, consequently, an induced effective interaction between the quasiparticles. Both of these quantities have an influence on the particle-hole (ph) as well as on the particle-particle (pp) channel.

For the calculation of the response of a nucleus in an external field we use the Bethe-Salpeter equation. It contains both the static and the dynamical effective interactions and it is formulated in the doubled two-quasiparticle basis of the Dirac-Hartree-BCS eigenstates. This Bethe-Salpether equation describes the quasiparticle-phonon coupling and pairing correlations on the equal footing. It is solved using the QTBA developed in Ref. [27], which allows the truncation to $2q \otimes$ phonon configurations and guarantees that the solution is positive definite. We also use the subtraction procedure introduced and justified in the Ref. [27]. As in the case without pairing it avoids double counting of the QPC. At zero energy, i.e., at the ground state, particle vibrational coupling should have no influence, because the correlations induced by QPC in the ground state have already been taken into account in the RHB description through the parameters of the energy functional initially fitted to reproduce experimental data, such as nuclear binding energies and radii. Therefore, the relativistic mean field contains effectively all the correlations in the static approximation. The energy dependence of the self-energy influences only excitations at finite energy in the nucleus.

In the present work we develop the relativistic quasiparticle time blocking approximation (RQTBA) and apply it for the description of electric dipole excitations in even-even spherical open-shell nuclei, such as the tin ($Z = 50$) isotopes ^{100,106,114,116,120,130}Sn and the ($N = 50$) isotones ^{88}Sr, ^{90}Zr, ^{92}Mo. The RQTBA method, whose physical content is an extension of the RQRPA by a coupling to low-lying collective vibrations, provides spectra enriched with the $2q \otimes$ phonon states. They cause a strong redistribution of the RQRPA strength. As a result, we obtain an additional broadening of the giant dipole resonance (GDR) and a spreading of the soft dipole mode (pygmy dipole resonance, PDR) to lower energies in the nuclei under investigation.

The article is organized as follows. In Sec. II we formulate basic relations of our approach in a rather general form. In Sec. II D we give a more detailed formalism for spherical nuclei in the form adapted for numerical calculations. Section III is devoted to the description of some numerical details and to the presentation of our results for even-even semi-magic nuclei. Finally, Sec. IV contains conclusions and an outlook.

II. GENERAL FORMALISM

A. Basic relations of the covariant density functional theory for nuclei with pairing

In this subsection we recall the general formalism of covariant density functional theory with pairing, introduce notations, and determine conventions used later on.

In open-shell nuclei, pairing correlations play an essential role and have to be incorporated consistently in a description of the ground state as well as of excited states, including many-body dynamics. Considering *pp* correlations in addition to the usual *ph* interaction, existing in normal systems, one has to provide a unified description of both *pp* and *ph* channels.

In contrast to Hartree- or Hartree-Fock theory, where *pp* correlations are neglected, and where the building blocks of excitations (the quasiparticles in the sense of Landau) are either nucleons in levels above the Fermi surface (particles) or missing nucleons in levels below the Fermi surface (holes), we have now quasiparticles in the sense of Bogoliubov that are described by a combination of creation and annihilation operators. This fact can be expressed in a standard way by introducing the following two-component operator, which is a generalization of the usual particle annihilation operator:

$$\Psi(1) = \begin{bmatrix} a(1) \\ a^\dagger(1) \end{bmatrix}. \tag{1}$$

Here $a(1) = e^{iHt_1} a_{k_1} e^{-iHt_1}$ is a nucleon annihilation operator in the Heisenberg picture and the quantum numbers k_1 represent an arbitrary basis, $1 = \{k_1, t_1\}$. To keep the notation simple we use in the following $1 = \{\boldsymbol{r}_1, t_1\}$ and omit spin and isospin indices.

Let us introduce the chronologically ordered product of the operator $\Psi(1)$ in Eq. (1) and its Hermitian conjugated operator $\Psi^\dagger(2)$, averaged over the ground state $|\Phi_0\rangle$ of the system that will be concretized below. This tensor of rank 2

$$G(1,2) = -i\langle\Phi_0|T\Psi(1)\Psi^\dagger(2)|\Phi_0\rangle \tag{2}$$

is the generalized Green's function that can be expressed through a 2×2 matrix:

$$\begin{aligned} G(1,2) = &-i\theta(t_1 - t_2)\langle\Phi_0| \begin{bmatrix} a(1)a^\dagger(2) & a(1)a(2) \\ a^\dagger(1)a^\dagger(2) & a^\dagger(1)a(2) \end{bmatrix} |\Phi_0\rangle \\ &+ i\theta(t_2 - t_1)\langle\Phi_0| \begin{bmatrix} a^\dagger(2)a(1) & a(2)a(1) \\ a^\dagger(2)a^\dagger(1) & a(2)a^\dagger(1) \end{bmatrix} |\Phi_0\rangle. \end{aligned} \tag{3}$$

Similar definitions for the Green's function in nonrelativistic superfluid systems have been used in Refs. [27,28,38,39]. Note that we define the definition of Green's functions here in the way of nonrelativistic many-body theory, which differs form the conventional definition $\langle T\Psi\bar{\Psi}\rangle$ adopted in relativistic field theories by the replacement of $\bar{\Psi}$ by $\Psi^\dagger$, i.e., by a Dirac matrix $\beta = \gamma_0$. This notation is more convenient for our analysis and the matrix β needed for Lorentz invariance is included in the vertices. Therefore the generalized density matrix is obtained as a limit

$$\mathcal{R}(\boldsymbol{r}_1, \boldsymbol{r}_2, t_1) = -i \lim_{t_2 \to t_1 + 0} G(1,2) \tag{4}$$

from the second term of Eq. (3), and, in the notation of Valatin [33], it can be expressed as a matrix of doubled dimension containing as components the normal density ρ and the abnormal density $\varkappa$, the so called pairing tensor:

$$\mathcal{R}(\boldsymbol{r}_1, \boldsymbol{r}_2, t) = \begin{bmatrix} \rho(\boldsymbol{r}_1, \boldsymbol{r}_2, t) & \varkappa(\boldsymbol{r}_1, \boldsymbol{r}_2, t) \\ -\varkappa^*(\boldsymbol{r}_1, \boldsymbol{r}_2, t) & \delta(\boldsymbol{r}_1 - \boldsymbol{r}_2) - \rho^*(\boldsymbol{r}_1, \boldsymbol{r}_2, t) \end{bmatrix}. \tag{5}$$

These densities play a key role in the description of a superfluid many-body system.

In covariant density functional theory for normal systems the ground state of the nucleus is a Slater determinant describing nucleons, which move independently in meson fields ϕ_m characterized by their quantum numbers for spin, parity, and isospin. In the present investigation we use the concept of conventional relativistic mean-field theory and include the σ-, ω-, and ρ-meson fields and the electromagnetic field as the minimal set of fields providing a rather good quantitative description of bulk and single-particle properties in the nucleus [1,40,41]. This means that the index m runs over the different types of fields $m = \{\sigma, \omega, \rho, A\}$. The summation over m implies in particular scalar products in Minkowski space for the vector fields and in isospace for the ρ field. To obtain a Lorentz invariant theory, these classical fields $\phi_m = \{\sigma, \omega^\mu, \vec{\rho}^\mu, A^\mu\}$ are generated in a self-consistent way by the exchange of virtual particles, called mesons, and the photon.

Finally, the energy depends in the case without pairing correlations on the normal density matrix ρ and the various fields ϕ_m:

$$\begin{aligned} E_{\mathrm{RMF}}[\rho, \phi] = \mathrm{Tr}[(\boldsymbol{\alpha}\mathbf{p} + \beta m)\rho] + \sum_m \Bigg\{ &\mathrm{Tr}[(\beta\Gamma_m\phi_m)\rho] \\ &\pm \int \left[\frac{1}{2}(\nabla\phi_m)^2 + U_m(\phi)\right] d^3r \Bigg\}. \end{aligned} \tag{6}$$

Here we have neglected retardation effects, i.e., time derivatives of the fields ϕ_m. The plus sign in Eq. (6) holds for scalar fields and the minus sign for vector fields. The trace operation implies a sum over Dirac indices and an integral in coordinate space. $\boldsymbol{\alpha}$ and β are Dirac matrices and the vertices Γ_m are given by

$$\begin{aligned} &\Gamma_\sigma = g_\sigma, \quad \Gamma^\mu_\omega = g_\omega\gamma^\mu, \quad \vec{\Gamma}^\mu_\rho = g_\rho\vec{\tau}\gamma^\mu, \\ &\Gamma^\mu_e = e\frac{(1-\tau_3)}{2}\gamma^\mu, \end{aligned} \tag{7}$$

with the corresponding coupling constants g_m for the various meson fields and for the electromagnetic field.

The quantities $U_m(\phi)$ are, in the case of a linear meson couplings, given by the term

$$U_m(\phi) = \tfrac{1}{2}m_m^2\phi_m^2 \tag{8}$$

containing the meson masses m_m. For nonlinear meson couplings, as, for instance, for the σ meson in the parameter set NL3 we have, as proposed in Ref. [42]:

$$U(\sigma) = \frac{1}{2}m_\sigma^2\sigma^2 + \frac{g_2}{3}\sigma^3 + \frac{g_3}{4}\sigma^4. \tag{9}$$

with two additional coupling constants g_2 and g_3.

In superfluid covariant density functional theory the energy is a functional of the Valatin density $\mathcal{R}$ and the fields ϕ_m. Therefore RHB theory can be derived from an energy

functional that depends on the normal density ρ and the abnormal density $\varkappa$ as well as on the meson and Coulomb fields ϕ_m. We use here a density functional of the form

$$E_{\rm RHB}[\rho,\varkappa,\varkappa^*,\phi] = E_{\rm RMF}[\rho,\phi] + E_{\rm pair}[\varkappa,\varkappa^*], \quad (10)$$

where the pairing energy is expressed by an effective interaction $\tilde{V}^{pp}$ in the pp channel:

$$E_{\rm pair}[\varkappa,\varkappa^*] = \tfrac{1}{4}\,{\rm Tr}\,[\varkappa^*\tilde{V}^{pp}\varkappa]. \quad (11)$$

Here and in the following a tilde sign is used to express the static character of a quantity, i.e., the fact that it does not depend on the energy. Of course, in Eq. (10) we could also use density-dependent pairing forces with $E_{\rm pair} = E_{\rm pair}[\rho,\varkappa]$ as it is done, for instance, in Refs. [43,44]. However, in the present investigation we do not consider this possibility. The effective interaction $\tilde{V}^{pp}$ in the particle-particle channel is supposed to be independent on the interaction in the particle-hole channel (see, e.g., Ref. [13]) mediated by the mesons and the electromagnetic fields determined above. Generally, the form of $\tilde{V}^{pp}$ is restricted only by the conditions of the relativistic invariance of $E_{\rm pair}$ with respect to the transformations of the abnormal densities (see Ref. [45]). In this section, we consider the general form of $\tilde{V}^{pp}$ as a nonlocal function in coordinate representation. In all the applications discussed in Sec. II D we use for $\tilde{V}^{pp}$ a simple monopole-monopole interaction.

The classical variational principle applied to the energy functional of Eq. (10)

$$\delta\int_{t_1}^{t_2}(\langle\Phi_0|i\partial_t|\Phi_0\rangle - E_{\rm RHB}[\rho,\varkappa,\varkappa^*,\phi])dt = 0 \quad (12)$$

leads to the equation of motion for the generalized density matrix $\mathcal{R}$:

$$i\partial_t\mathcal{R} = [\mathcal{H}_{\rm RHB}(\mathcal{R}),\mathcal{R}] \quad (13)$$

with the RHB Hamiltonian

$$\mathcal{H}_{\rm RHB} = 2\frac{\delta E_{\rm RHB}}{\delta\mathcal{R}} = \begin{pmatrix} h^{\mathcal{D}} - m - \lambda & \Delta \\ -\Delta^* & -h^{\mathcal{D}*} + m + \lambda \end{pmatrix}, \quad (14)$$

where λ is the chemical potential (counted from the continuum limit). In the static case we find

$$[\mathcal{H}_{\rm RHB}(\mathcal{R}),\mathcal{R}] = 0. \quad (15)$$

Because of time reversal invariance the currents vanish and we obtain the single nucleon Dirac Hamiltonian

$$h^{\mathcal{D}} = \boldsymbol{\alpha}\mathbf{p} + \beta(m + \tilde{\Sigma}) \quad (16)$$

with the RMF self-energy

$$\tilde{\Sigma}(\boldsymbol{r}) = \sum_m \Gamma_m\phi_m(r). \quad (17)$$

The pairing field Δ reads in this case:

$$\Delta(\boldsymbol{r},\boldsymbol{r}') = \frac{1}{2}\int d\boldsymbol{r}''d\boldsymbol{r}'''\tilde{V}^{pp}(\boldsymbol{r},\boldsymbol{r}',\boldsymbol{r}'',\boldsymbol{r}''')\varkappa(\boldsymbol{r}'',r'''). \quad (18)$$

Equation (15) leads to the relativistic Hartree-Bogoliubov equations [35]

$$\mathcal{H}_{\rm RHB}\big|\psi_k^\eta\big\rangle = \eta E_k\big|\psi_k^\eta\big\rangle, \eta = \pm 1, \quad (19)$$

where $|\psi_k^\eta\rangle$ are the eigenfunctions corresponding to eigenvalues ηE_k. They are the 8-dimensional Bogoliubov-Dirac spinors of the following form

$$|\psi_k^+(\boldsymbol{r})\rangle = \begin{bmatrix} U_k(\boldsymbol{r}) \\ V_k(\boldsymbol{r}) \end{bmatrix}, \quad |\psi_k^-(\boldsymbol{r})\rangle = \begin{bmatrix} V_k^*(\boldsymbol{r}) \\ U_k^*(\boldsymbol{r}) \end{bmatrix}. \quad (20)$$

Note that the index k labels here and in the following quasiparticles in contrast to the index k_1 used after Eq. (1) for the particle basis.

The generalized density matrix is obtained as follows:

$$\mathcal{R}(\boldsymbol{r},\boldsymbol{r}') = \sum_k |\psi_k^-(\boldsymbol{r})\rangle\langle\psi_k^-(\boldsymbol{r}')|, \quad (21)$$

where the summation is performed only over the states having large upper components of the Dirac spinors [i.e., large functions $f_{(k)}(r)$ in Eq. (A1) below]. This restriction corresponds to the so-called *no-sea approximation* (see Ref. [37]).

The behavior of the meson and Coulomb fields is derived from the energy functional (10) by variation with respect to the fields ϕ_m. We obtain Klein-Gordon equations. In the static case they have the form

$$-\Delta\phi_m(\boldsymbol{r}) + U'[\phi_m(\boldsymbol{r})] = \mp\sum_k V_k^T(\boldsymbol{r})\beta\Gamma_m V_k^*(\boldsymbol{r}). \quad (22)$$

Equation (22) determines the potentials entering the single-nucleon Dirac Hamiltonian (16) and is solved self-consistently together with Eq. (19). The system of Eqs. (19) and (22) determine the ground state of an open-shell nucleus in the relativistic Hartree-Bogoliubov approach.

Neglecting the small effects of the pairing cut-off, the Hartree-Bogoliubov theory with a monopole-monopole force, as it is used in the present investigation, is equivalent to Hartree-BCS approximation, where the Dirac hamiltonian $h^{\mathcal{D}}$ (16) and the normal nucleon density are diagonal. In this case the spinors (20) are expressed through eigenvectors of the operator $h^{\mathcal{D}}$, see Eq. (A13) of the Appendix A. Below we formulate our approach in the space of these eigenvectors which we call Dirac-Hartree-BCS (DHBCS) basis and use indices k or k_i, $i = 1, 2, \ldots$ for the set of quantum numbers in this basis.

B. Quasiparticle-vibration coupling as a model for an energy dependence of the single-quasiparticle self-energy

The single quasiparticle equation of motion (19) determines the behavior of a nucleon with a static self-energy. To include dynamics, i.e., a more realistic time dependence in the self-energy one has to extend the energy functional by an appropriate term leading to a self-energy (17) with time dependence. In the present work we use for this purpose the successful but relatively simple particle-vibration coupling model introduced in Refs. [32,46]. Following the general logic of this model, we consider the total single-nucleon self-energy for the Green's function defined in Eq. (2) as a sum of the RHB self-energy and an energy-dependent nonlocal term in the doubled space:

$$\Sigma(\boldsymbol{r},\boldsymbol{r}';\varepsilon) = \tilde{\Sigma}(\boldsymbol{r},\boldsymbol{r}') + \Sigma^{(e)}(\boldsymbol{r},\boldsymbol{r}';\varepsilon) \quad (23)$$

with

$$\tilde{\Sigma}(\boldsymbol{r},\boldsymbol{r}') = \begin{bmatrix} \beta\tilde{\Sigma}(\boldsymbol{r})\delta(\boldsymbol{r}-\boldsymbol{r}') & \Delta(\boldsymbol{r},\boldsymbol{r}') \\ -\Delta^*(\boldsymbol{r},\boldsymbol{r}') & -\beta\tilde{\Sigma}^*(\boldsymbol{r})\delta(\boldsymbol{r}-\boldsymbol{r}') \end{bmatrix}. \quad (24)$$

The energy-dependent operator $\Sigma^{(e)}(\boldsymbol{r},\boldsymbol{r}';\varepsilon)$ will be determined below (the upper index e in this quantity indicates the energy dependence). The Dyson equation for the single-quasiparticle Green's function (2) in the doubled space has the following form:

$$[\varepsilon - \mathcal{H}_{\mathrm{RHB}} - \Sigma^{(e)}(\varepsilon)]G(\varepsilon) = 1. \quad (25)$$

To study the influence of the energy-dependent part of the self-energy on the single-quasiparticle energies we formulate Eq. (25) in the DHBCS basis diagonalizing the Dirac Hamiltonian $h^{\mathcal{D}}$ of Eq. (16):

$$\sum_{\eta=\pm1}\sum_{k}\left[(\varepsilon-\eta_1 E_{k_1})\delta_{\eta_1\eta}\delta_{k_1k} - \Sigma^{(e)\eta_1\eta}_{k_1k}(\varepsilon)\right]G^{\eta\eta_2}_{kk_2}(\varepsilon) = \delta_{\eta_1\eta_2}\delta_{k_1k_2}, \quad (26)$$

where

$$\Sigma^{(e)\eta_1\eta_2}_{k_1k_2}(\varepsilon) = \int d^3r d^3r' \left\langle \psi^{\eta_1}_{k_1}(\boldsymbol{r})\right| \Sigma^{(e)}(\boldsymbol{r},\boldsymbol{r}';\varepsilon) \left|\psi^{\eta_2}_{k_2}(\boldsymbol{r}')\right\rangle, \quad (27)$$

$$G^{\eta_1\eta_2}_{k_1k_2}(\varepsilon) = \int d^3r d^3r' \left\langle \psi^{\eta_1}_{k_1}(\boldsymbol{r})\right| G(\boldsymbol{r},\boldsymbol{r}';\varepsilon) \left|\psi^{\eta_2}_{k_2}(\boldsymbol{r}')\right\rangle. \quad (28)$$

In this basis the single-quasiparticle Green's function $\tilde{G}$ of the static mean field has the following simple diagonal form:

$$\tilde{G}^{\eta_1\eta_2}_{k_1k_2}(\varepsilon) = \delta_{k_1k_2}\delta_{\eta_1\eta_2}\tilde{G}^{\eta_1}_{k_1}(\varepsilon),$$
$$\tilde{G}^{\eta_1}_{k_1}(\varepsilon) = \frac{1}{\varepsilon - \eta_1 E_{k_1} + i\eta_1\delta}, \delta \to +0. \quad (29)$$

As in Refs. [18,21], we use the particle-phonon coupling model for the energy-dependent part of the self-energy $\Sigma^{(e)}$. In the DHBCS basis its matrix elements are given by:

$$\Sigma^{(e)\eta_1\eta_2}_{k_1k_2}(\varepsilon) = \sum_{\eta=\pm1}\sum_{\eta_\mu=\pm1}\sum_{k,\mu}\frac{\delta_{\eta_\mu,\eta}\gamma^{\eta_\mu;\eta_1\eta}_{\mu;k_1k}\gamma^{\eta_\mu;\eta_2\eta*}_{\mu;k_2k}}{\varepsilon - \eta E_k - \eta_\mu(\Omega_\mu - i\delta)}, \quad \delta \to +0. \quad (30)$$

The index k formally runs over all single-quasiparticle states, including antiparticle states with negative energies. In the doubled quasiparticle space we can no longer distinguish occupied and unoccupied states considering that all the orbits are partially occupied. But in practical calculations, it is assumed that there are no pairing correlations in the Dirac sea [37] and the orbits with negative energies are treated in the no-sea approximation. As it has been shown in calculations for nuclei with closed shells in Ref. [18], the numerical contribution of the diagrams with intermediate states k with negative energies is very small due to the large energy denominators in the corresponding terms of the self-energy (30). The index μ in Eq. (30) labels the set of phonons taken into account. Ω_μ are their frequencies and $\eta_\mu = \pm1$ labels forward and backward going diagrams in Eq. (30). The vertices $\gamma^{\eta_\mu;\eta_1\eta_2}_{\mu;k_1k_2}$ determine the coupling of the quasiparticles to the collective state μ:

$$\gamma^{\eta_\mu;\eta_1\eta_2}_{\mu;k_1k_2} = \delta_{\eta_\mu,+1}\gamma^{\eta_1\eta_2}_{\mu;k_1k_2} + \delta_{\eta_\mu,-1}\gamma^{\eta_2\eta_1*}_{\mu;k_2k_1}. \quad (31)$$

In the conventional version of the particle-vibrational coupling model the phonon vertices γ_μ are derived from the corresponding transition densities $\mathcal{R}_\mu$ and the static effective interaction:

$$\gamma^{\eta_1\eta_2}_{\mu;k_1k_2} = \sum_{k_3k_4}\sum_{\eta_3\eta_4}\tilde{V}^{\eta_1\eta_4,\eta_2\eta_3}_{k_1k_4,k_2k_3}\mathcal{R}^{\eta_3\eta_4}_{\mu;k_3k_4}, \quad (32)$$

where $\tilde{V}^{\eta_1\eta_4,\eta_2\eta_3}_{k_1k_4,k_2k_3}$ denotes a relativistic matrix element of the static residual interaction in the doubled space. It is obtained as a functional derivative of the relativistic mean-field self-energy $\tilde{\Sigma}$ with respect to the relativistic generalized density matrix $\mathcal{R}$:

$$\tilde{V}^{\eta_1\eta_4,\eta_2\eta_3}_{k_1k_4,k_2k_3} = \frac{\delta\tilde{\Sigma}^{\eta_4\eta_3}_{k_4k_3}}{\delta\mathcal{R}^{\eta_2\eta_1}_{k_2k_1}}. \quad (33)$$

The transition densities $\mathcal{R}_\mu$ are defined by the time dependence of the generalized density (5)

$$\mathcal{R}(t) = \mathcal{R}_0 + \sum_\mu(\mathcal{R}_\mu e^{i\Omega_\mu t} + \mathrm{h.c.}) \quad (34)$$

describing the oscillating system. We use the linearized version of the model that assumes that the transition densities $\mathcal{R}_\mu$ are not influenced by the particle-phonon coupling and that they can be computed within the relativistic QRPA. In the linearized version of the QPC model we solve the RQRPA equations for transition densities

$$\mathcal{R}^{\eta}_{\mu;k_1k_2} = \tilde{R}^{(0)\eta}_{k_1k_2}(\Omega_\mu)\sum_{k_3k_4}\sum_{\eta'}\tilde{V}^{\eta\eta'}_{k_1k_4,k_2k_3}\mathcal{R}^{\eta'}_{\mu;k_3k_4}, \quad (35)$$

where

$$\mathcal{R}^{\eta}_{\mu;k_1k_2} = \mathcal{R}^{\eta,-\eta}_{\mu;k_1k_2}, \quad \tilde{R}^{(0)\eta}_{k_1k_2}(\omega) = \tilde{R}^{(0)\eta,-\eta}_{k_1k_2}(\omega),$$
$$\tilde{V}^{\eta\eta'}_{k_1k_4,k_2k_3} = \tilde{V}^{\eta,-\eta',-\eta,\eta'}_{k_1k_4,k_2k_3}, \quad (36)$$

which means that we cut out certain components of the tensors in the quasiparticle space. The quantity $\tilde{R}$ is, as usual, the two-quasiparticle propagator, or the mean-field response function, which is a convolution of two single-quasiparticle mean-field Green's functions (29):

$$\tilde{R}^{(0)\eta}_{k_1k_2}(\omega) = \frac{1}{\eta\omega - E_{k_1} - E_{k_2}}. \quad (37)$$

In Eq. (35) we use the static quasiparticle-interaction $\tilde{V}$ of Eq. (33). Of course, in general, we should calculate these transition densities taking into account also the additional energy-dependent residual interaction $V^{(e)}$ [see Eq. (44) below] in a self-consistent iteration procedure. However, this is not done in the investigations presented here.

C. Response function in the quasiparticle time-blocking approximation

Now we have to formulate the Bethe-Salpeter equation (BSE) for the response of a superfluid nucleus in a weak external field. The method to derive the BSE for superfluid nonrelativistic systems from a generating functional is known and can be found, e.g., in Ref. [27] where the generalized Green's function formalism was used. Applying the same technique in the relativistic case, one obtains a similar ansatz for the BSE. In full analogy to the case without pairing

described in Ref. [21] it is convenient to begin the derivation in the time representation. Let us therefore include the time variable and the variable η defined in Eq. (19), which distinguishes components in the doubled quasiparticle space, into the single-quasiparticle indices using $1 = \{k_1, \eta_1, t_1\}$. In this notation the BSE for the response function R reads:

$$R(14,23) = G(1,3)G(4,2) - i\sum_{5678} G(1,5)G(6,2)V(58,67)R(74,83), \quad (38)$$

where the summation over the number indices 1, 2, ... implies integration over the respective time variables. The function G is the exact single-quasiparticle Green's function and V is the amplitude of the effective interaction irreducible in the ph channel. This amplitude is determined as a variational derivative of the full self-energy Σ with respect to the exact single-quasiparticle Green's function:

$$V(14,23) = i\frac{\delta\Sigma(4,3)}{\delta G(2,1)}. \quad (39)$$

Similar as in Ref. [21], we introduce the free response $R^0(14,23) = G(1,3)G(4,2)$ and formulate the Bethe-Salpeter equation (38) in a shorthand notation, omitting the number indices:

$$R = R^0 - iR^0VR. \quad (40)$$

For the sake of simplicity, we will use this shorthand notation in the following discussions. Because the self-energy in Eq. (23) has two parts $\Sigma = \tilde{\Sigma} + \Sigma^{(e)}$, the effective interaction V in Eq. (38) is a sum of the static RMF interaction $\tilde{V}$ and the energy-dependent term $V^{(e)}$:

$$V = \tilde{V} + V^{(e)}, \quad (41)$$

where (with $t_{12} = t_1 - t_2$)

$$\tilde{V}(14,23) = \tilde{V}^{\eta_1\eta_4,\eta_2\eta_3}_{k_1k_4,k_2k_3}\delta(t_{31})\delta(t_{21})\delta(t_{34}), \quad (42)$$

$$V^{(e)}(14,23) = i\frac{\delta\Sigma^{(e)}(4,3)}{\delta G(2,1)}, \quad (43)$$

and $\tilde{V}^{\eta_1\eta_4,\eta_2\eta_3}_{k_1k_4,k_2k_3}$ is determined by Eq. (33). In the DHBCS basis the Fourier transform of the amplitude $V^{(e)}$ has the form:

$$V^{(e)\eta_1\eta_4,\eta_2\eta_3}_{k_1k_4,k_2k_3}(\omega,\varepsilon,\varepsilon') = \sum_{\mu,\eta_\mu}\frac{\eta_\mu\gamma^{\eta_\mu;\eta_3\eta_1*}_{\mu;k_3k_1}\gamma^{\eta_\mu;\eta_4\eta_2}_{\mu;k_4k_2}}{\varepsilon - \varepsilon' + \eta_\mu(\Omega_\mu - i\delta)}, \quad \delta\to+0. \quad (44)$$

To make the Bethe-Salpeter equation (40) more convenient for the further analysis we eliminate the exact Green's function G and rewrite it in terms of the mean field Green's function $\tilde{G}$ which is diagonal in the DHBCS basis. In time representation we have the following ansatz:

$$\tilde{G}(1,2) = -i\eta_1\delta_{k_1k_2}\delta_{\eta_1\eta_2}\theta(\eta_1\tau)e^{-i\eta_1E_{k_1}\tau}, \quad \tau = t_1 - t_2, \quad (45)$$

and its Fourier transform is given by Eq. (29).

Using the connection between the mean field GF $\tilde{G}$ and the exact GF G in the Nambu form

$$\tilde{G}^{-1}(1,2) = G^{-1}(1,2) + \Sigma^{(e)}(1,2), \quad (46)$$

one can eliminate the unknown exact GF G from the Eq. (40) and rewrite it as follows:

$$R = \tilde{R}^0 - i\tilde{R}^0WR \quad (47)$$

with the mean-field response $\tilde{R}^0(14,23) = \tilde{G}(1,3)\tilde{G}(4,2)$, and W is a new interaction of the form

$$W = \tilde{V} + W^{(e)}, \quad (48)$$

where

$$W^{(e)}(14,23) = V^{(e)}(14,23) + i\Sigma^{(e)}(1,3)\tilde{G}^{-1}(4,2) + i\tilde{G}^{-1}(1,3)\Sigma^{(e)}(4,2) - i\Sigma^{(e)}(1,3)\Sigma^{(e)}(4,2). \quad (49)$$

Thus, we have obtained the BSE in terms of the mean-field propagator, containing the well-known mean-field Green's functions $\tilde{G}$ and a rather complicated effective interaction W in Eq. (48), which, however, is also expressed through the mean-field Green's functions.

Then, we apply the quasiparticle time blocking approximation to the Eq. (47) employing the time projection operator in the integral part of this equation. In our case this procedure is a combination of the nonrelativistic QTBA [27] with the relativistic version of this method [21] developed for the systems without pairing correlations. The time projection leads, after some algebra and the transformation to the energy domain, to an algebraic equation for the response function. For the ph-type components of the response function it has the form:

$$R^{\eta\eta'}_{k_1k_4,k_2k_3}(\omega) = \tilde{R}^{(0)\eta}_{k_1k_2}(\omega)\delta_{k_1k_3}\delta_{k_2k_4}\delta_{\eta\eta'} + \tilde{R}^{(0)\eta}_{k_1k_2}(\omega) \times \sum_{k_5k_6k_7k_8}\sum_{\eta''}\bar{W}^{\eta\eta''}_{k_5k_8,k_6k_7}(\omega)R^{\eta''\eta'}_{k_7k_4,k_8k_3}(\omega), \quad (50)$$

where

$$R^{\eta\eta'}_{k_1k_4,k_2k_3}(\omega) = R^{\eta,-\eta',-\eta,\eta'}_{k_1k_4,k_2k_3}(\omega), \quad (51)$$

$$R^{\eta_1\eta_4,\eta_2\eta_3}_{k_1k_4,k_2k_3}(\omega) = -i\int_{-\infty}^{\infty}dt_1dt_2dt_3dt_4\delta(t_1-t_2)\delta(t_3-t_4) \times \delta(t_4)e^{i\omega t_{13}}R(14,23), \quad (52)$$

$$\bar{W}^{\eta\eta'}_{k_1k_4,k_2k_3}(\omega) = \tilde{V}^{\eta\eta'}_{k_1k_4,k_2k_3} + \left(\Phi^{\eta}_{k_1k_4,k_2k_3}(\omega) - \Phi^{\eta}_{k_1k_4,k_2k_3}(0)\right)\delta_{\eta\eta'}. \quad (53)$$

In Eq. (53) $\Phi(\omega)$ is the dynamical part of the interaction amplitude in the QTBA responsible for the particle-phonon coupling with the following forward ($\eta = 1$) and backward ($\eta = -1$) components:

$$\Phi^{\eta}_{k_1k_4,k_2k_3}(\omega) = \sum_{\mu}\left[\delta_{k_1k_3}\sum_{k_6}\frac{\gamma^{-\eta}_{\mu;k_6k_2}\gamma^{-\eta*}_{\mu;k_6k_4}}{\eta\omega - E_{k_1} - E_{k_6} - \Omega_\mu} + \delta_{k_2k_4}\sum_{k_5}\frac{\gamma^{\eta}_{\mu;k_1k_5}\gamma^{\eta*}_{\mu;k_3k_5}}{\eta\omega - E_{k_5} - E_{k_2} - \Omega_\mu} - \left(\frac{\gamma^{\eta}_{\mu;k_1k_3}\gamma^{-\eta*}_{\mu;k_2k_4}}{\eta\omega - E_{k_3} - E_{k_2} - \Omega_\mu} + \frac{\gamma^{\eta*}_{\mu;k_3k_1}\gamma^{-\eta}_{\mu;k_4k_2}}{\eta\omega - E_{k_1} - E_{k_4} - \Omega_\mu}\right)\right], \quad (54)$$

where we denote $\gamma^{\eta}_{\mu;k_1k_2} = \gamma^{\eta\eta}_{\mu;k_1k_2}$. Indices k_i in this expression formally run over the whole DHBCS space, but in applications we usually consider that the amplitude $\Phi^{\eta}_{k_1k_4,k_2k_3}(\omega)$ describes phonon coupling only within some energy window around the Fermi surface. It implies that this amplitude contains no antiparticle-quasiparticle (αq) configurations.

Notice, that in our approach we cut out only the components without ground state correlations (GSC) induced by phonon coupling that include the main contribution of the phonon coupling and neglect some more delicate terms. However, ground-state correlations of the QRPA type are taken into account due to the presence of the $\tilde{V}^{\eta\eta'}_{k_1k_4,k_2k_3}$ terms of the static interaction in Eq. (50). By definition, the propagator $R(\omega)$ in Eq. (50) contains only configurations that are not more complicated than $2q \otimes$ phonon.

In Eq. (50) we have included the subtraction procedure because of the same reasons as in the Ref. [21]. Because the RMF ground state is adjusted to experimental data, it contains effectively many correlations in the static approximation and, in particular, also admixtures of phonons. Therefore, when we include them explicitly in the dynamics, this static part should be subtracted from the effective interaction to avoid double counting of the QPC correlations. Because the parameters of the density functional and, as a consequence, the effective interaction $\tilde{V}$ are adjusted to experimental ground-state properties at the energy $\omega = 0$, this part of the interaction $\Phi(\omega)$, which is already contained in $\tilde{V}$, is given by $\Phi(0)$. This subtraction method has been introduced in the Ref. [27] for self-consistent schemes.

Eventually, to describe the observed spectrum of the excited nucleus in a weak external field P as, for instance, an electromagnetic field, one needs to calculate the strength function:

$$S(E) = -\frac{1}{\pi} \lim_{\Delta\to+0} Im\Pi(E + i\Delta), \tag{55}$$

expressed through the polarizability $\Pi(\omega)$ defined as

$$\Pi(\omega) = \frac{1}{2} P^{\dagger} R(\omega) P := \frac{1}{2} \sum_{k_1k_2k_3k_4} \sum_{\eta\eta'} P^{\eta *}_{k_1k_2} R^{\eta\eta'}_{k_1k_4,k_2k_3}(\omega) P^{\eta'}_{k_3k_4}. \tag{56}$$

The imaginary part Δ of the energy variable is introduced for convenience to obtain a more smoothed envelope of the spectrum. This parameter has the meaning of an additional artificial width for each excitation. This width emulates effectively contributions from configurations that are not taken into account explicitly in our approach.

In relativistic RPA and QRPA calculations the Dirac sea plays an important role. A consistent derivation of relativistic RPA (QRPA) as the small amplitude limit of time-dependent RMF (RHB) theory in Ref. [12] shows that one has to include in addition to the usual ph configurations also antiparticle-hole (αh) configurations. Otherwise current conservation is violated [47] and the position of giant resonances cannot be described properly in relativistic RPA [48]. However, this increases the number of configurations dramatically as compared to nonrelativistic QRPA calculations and requires, in particular, in deformed relativistic QRPA calculations [49] an extremely large numerical effort. Recently, a simple method was proposed to avoid this problem. As discussed in Ref. [50], the *static no-sea* (SNS) approximation takes the contributions of the empty Dirac sea into account in a very good approximation by a renormalization of the total effective interaction $\bar{W}(\omega)$ in the Bethe-Salpeter equation.

D. Application of the approach: calculation scheme

The formulated relativistic QTBA is applied to calculations of the dipole strength in spherical nuclei with pairing. In this application we mainly follow the calculation scheme employed in Ref. [21,22], however, with some considerable modifications accounting pairing effects: all the equations are solved in the doubled space. The computation is performed by the following main steps:

(i) To calculate ground-state properties the Dirac equation (A7) together with the BCS equation (A11) for single nucleons are solved simultaneously with the Klein-Gordon equation (22) for meson fields in a self-consistent way to obtain the single-quasiparticle basis, which is the Dirac-Hartree-BCS basis, see Appendix A for details.

(ii) The RQRPA equations (35) with the static interaction $\tilde{V}$ of Eq. (33) are solved in the Dirac-Hartree-BCS basis to determine the low-lying collective vibrations (phonons), their energies and amplitudes. Details of the solution for a spherically symmetric case are given in Appendix B. The two sets of quasiparticles and phonons form the multitude of $2q \otimes$ phonon configurations which enter the quasiparticle-phonon coupling amplitude $\Phi(\omega)$ in Eq. (54).

(iii) The equation for the response function (50) is solved using this additional amplitude in the effective interaction $\bar{W}(\omega)$ (53). In Appendix C we give this equation in a coupled form for a given multipolarity formulated in the momentum-channel representation. Making a double convolution of the response function with the external field operator P, one obtains the polarizability (56) and the strength function (55) determining the spectrum of the nucleus.

III. COMPUTATIONAL DETAILS, RESULTS, AND DISCUSSION

A. Numerical details

For this first application we have chosen two chains of spherical even-even semimagic nuclei: one chain with $Z = 50$ and another one with $N = 50$. We have calculated the isovector dipole spectrum in the giant dipole resonance region and in the low-lying energy region in the two approximations: RQRPA and RQTBA for the quasiparticle-vibration coupling. All the results presented below have been obtained with making use of the NL3 parameter set [51] for the covariant density functional (6).

In the present work, pairing correlations were treated in the BCS approximation where the single-quasiparticle wave functions diagonalize the single-nucleon density matrix ρ. As pairing interaction we use the simple monopole-monopole form (B8) within the smoothed energy window with the

parameters $w = 20$ MeV, $d = 1$ MeV. The parameter G was chosen in such a way that the resulting gap at the Fermi surface reproduces the empirical gap expressed by the well known three-point formula:

$$\Delta^{(3)}_{N_\tau} = -\frac{(-1)^{N_\tau}}{2}[B(N_\tau - 1) + B(N_\tau + 1) - 2B(N_\tau)], \quad (57)$$

where $B(N_\tau)$ is the experimentally known binding energy of the nucleus with N_τ nucleons in the subsystem with pairing correlations (neutrons or protons). The RMF plus BCS equations are solved by expanding the nucleon spinors in a spherical harmonic oscillator basis [3]. In the present calculation we have used the basis of 20 oscillator shells.

In solving the RQRPA Eq. (B1) we have used the method proposed in Ref. [52] for a reduction of the eigenvalue problem by the generalized Cholesky decomposition. In the RQRPA as well as RQTBA calculations both Fermi and Dirac subspaces were truncated at energies far away from the Fermi surface: in the present work as well as in the Refs. [21,22] we fix the limits $E_{2q} < 100$ MeV and $E_{\alpha q} > -1800$ MeV with respect to the positive continuum (so far from the Fermi surface there are no pairing effects, therefore we have there pure particles and holes). A small artificial width was introduced as an imaginary part of the energy variable $\hbar\omega$ to have a smooth envelope of the calculated curves. In the calculations for tin isotopes we took 200 keV smearing for the spectrum in the wide energy region 0–30 MeV and 20 keV for the low-lying portion of the same spectrum below 10 MeV to distinguish its fine structure. For the $N = 50$ isotopes we used the smearing 400 keV, assuming the more pronounced contribution of the single-particle continuum in the GDR region, and 10 keV for the low-lying strength.

The energies and amplitudes of the most collective phonon modes with spin and parity $2^+, 3^-, 4^+, 5^-, 6^+$ have been calculated with the same restrictions and selected using the same criterion as in the Refs. [21,22] and in many other non-relativistic investigations in this context. Only the phonons with energies below the neutron separation energy for the investigated tin isotopes and below 10 MeV—for the $N = 50$ nuclei enter the phonon space because the contributions of the higher-lying modes are supposed to be small. Our previous experience within the nonrelativistic approach of Ref. [28] without the restriction of the phonon space by the energy has shown that the inclusion of the high-lying modes into the phonon space causes the change of the mean energies and widths of the resonances comparable with the smearing parameter (imaginary part of the energy variable) used in the calculations, because the physical sense of this parameter is to emulate contributions of remaining configurations which are not taken into account explicitly.

As a test of numerical correctness of our codes, the response equation has been solved both in the DHBCS basis and in momentum-channel space and identical results have been obtained. Because the quasiparticle-phonon coupling amplitude (C4) has a pole structure, its contributions to the final result for the strength function decrease considerably when we go away from the Fermi surface. Therefore, this coupling has been taken into account only within the $2q$-energy window $E_{2q} \leqslant 25$ MeV around the Fermi surface. This restriction means that above this energy we have no poles induced by the complex configurations and obtain the pure RQRPA poles, but with larger strength that comes from the integral contribution of the lower-lying energy spectrum. It has been checked that a further increase of this window does not influence considerably the strength functions at energies below the value of this window.

Although a large number of configurations of the $2q \otimes$ phonon type are taken into account explicitly in our approach, nevertheless we stay in the same two-quasiparticle space as in the RQRPA, therefore the problem of completeness of the phonon basis does not arise and, therefore, the phonon subspace and the subspace of the $2q \otimes$ phonon states can be truncated in the above-mentioned way. Another essential point is, that on all three stages of our calculations the same relativistic nucleon-nucleon static interaction $\tilde{V}$ has been employed. The vertices (B9) entering the QPC energy-dependent interaction are calculated with the same force. Therefore no further parameters are needed, and our calculation scheme is fully consistent.

The subtraction procedure developed in the Ref. [27] for self-consistent schemes has been incorporated in our approach. As it was mentioned above, this procedure removes the static contribution of the quasiparticle-phonon coupling from the static interaction in the ph channel. Therefore, the QPC interaction takes into account only the additional energy dependence introduced by the dynamics of the system. It has been found in the present calculations as well as in the calculations of the Ref. [28] that within the relatively large energy interval (0–30 MeV) the subtraction procedure provides a rather small but noticeable increase of the mean energy of the giant dipole resonance (about 0.7 MeV for tin region) and gives rise to the change by a few percents in the sum rule. Notice that the absolute value of the energy shift produced by the subtraction of $\Phi(0)$ in Eq. (53) is comparable with but not equal exactly to the absolute value of the shift produced by the dynamical part of the interaction amplitude $\Phi(\omega)$ which always reduces the mean energy of the resonance. The subtraction procedure restores the response at zero energy and, therefore, it does not disturb the symmetry properties of the RQRPA calculations. The zero energy modes connected with the spontaneous symmetry breaking in the mean-field solutions, as, for instance, the translational mode in the dipole case, remain at exactly the same positions after the inclusion of the quasiparticle-vibration coupling. In practice, however, because of the limited number of oscillator shells in our calculations this state is found already in the RQRPA without the QPC at a few hundreds keV above zero. In cases, where the results depend strongly on a proper separation of this spurious state, as, for instance, for investigations of the pygmy dipole resonance in neutron rich systems, we have to include a large number of the $2q$ configurations in the RQRPA solution to avoid mixing of the spurious state with the low-lying physical states.

B. Isovector dipole strength distribution: pygmy and giant resonances

In Figs. 1 and 2 the calculated dipole spectra for the tin isotopes ^{100}Sn, ^{106}Sn, ^{114}Sn and ^{116}Sn, ^{120}Sn, ^{130}Sn,

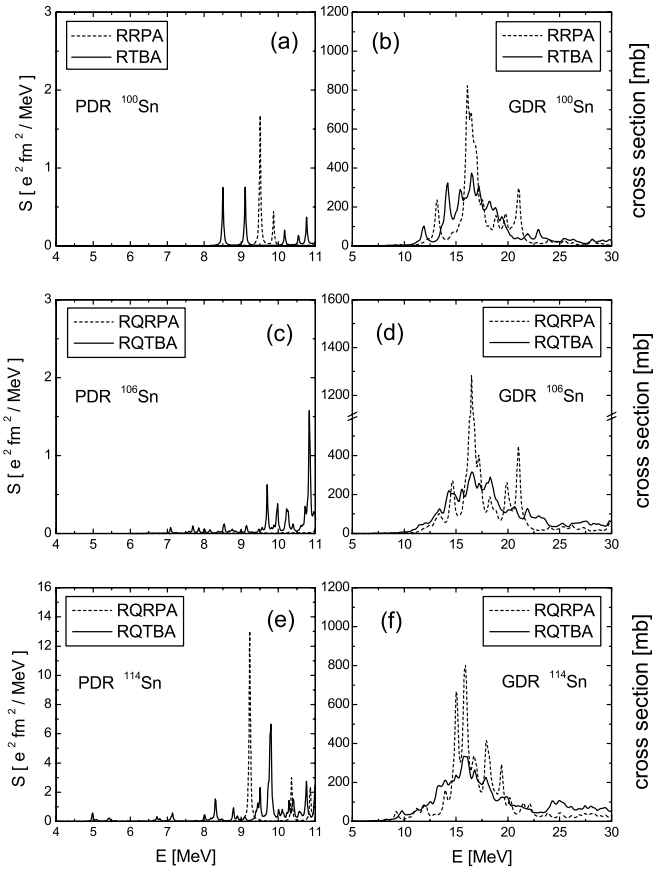

FIG. 1. The calculated dipole spectra for the light tin isotopes ^{100}Sn, ^{106}Sn, ^{114}Sn. Photo absorption cross sections computed with the artificial width 200 keV (b, d, f). The low-lying portions of the corresponding spectra in terms of the strength function, calculated with 20-keV smearing (a, c, e). Calculations within the RQRPA are shown by the dashed curves, and the RQTBA by the solid curves.

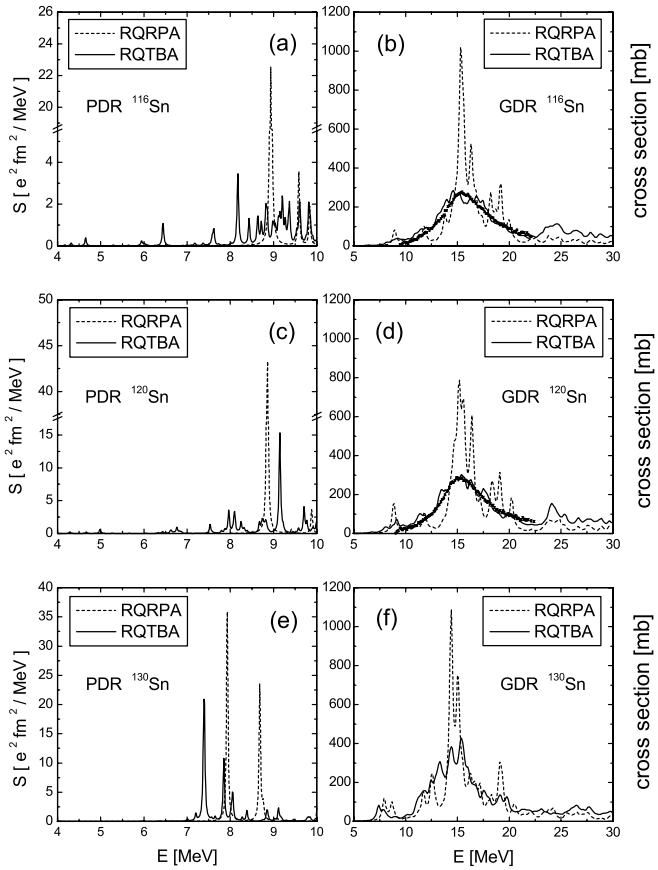

FIG. 2. The same as in Fig. 1, but for heavier tin isotopes ^{116}Sn, ^{120}Sn, ^{130}Sn, compared to data of Ref. [53] for ^{116,120}Sn shown by black circles with bars.

respectively, are given. The right panels of the figures show the photo absorption cross section

$$\sigma_{E1}(E) = \frac{16\pi^3 e^2}{9\hbar c} E\, S_{E1}(E), \tag{58}$$

which is determined by the dipole strength function S_{E1}, calculated with the usual isovector dipole operator. The left panels show the low-lying parts of the corresponding spectrum in terms of the strength function, calculated with the small imaginary part for the energy variable, to see the fine structure of the spectrum and sometimes individual levels in this region. Figure 3 represents the analogous results for the three $N = 50$ nuclei: ^{88}Sr, ^{90}Zr, and ^{92}Mo. Calculations within the RQRPA are shown by the dashed curves, and the RQTBA by the solid curves. Experimental data are taken from the EXFOR database [53].

These three figures clearly demonstrate how the two-quasiparticle states, which are responsible for the spectrum of the RQRPA excitations, are fragmented through the coupling to the collective vibrational states. The effect of the particle-vibration coupling on the low-lying dipole strength below and around the neutron threshold within the presented approach is shown in the left panels of the Figs. 1–3. Our calculations for the tin chain give us an example how the low-lying strength develops with the increase of the neutron excess. In the doubly magic ^{100}Sn two first relatively weak RRPA peaks appear between 9 and 10 MeV. Quasiparticle-phonon coupling redistributes these structures and shifts them about one MeV lower. In the ^{106}Sn due to the pairing correlations in the neutron system the whole RQRPA picture is shifted toward higher energies, and there is practically no strength below 10 MeV. In the corresponding figure we find only the strength caused by the fragmentation of the higher-lying RQRPA peaks above 11 MeV. In the ^{114}Sn the neutron excess becomes enough to form the pronounced pygmy mode situated in the RQRPA at about 9.2 MeV and spread over many states of the $2q \otimes$ phonon nature beginning from 5 MeV. Figure 2 shows how this tendency develops in the more neutron-rich nuclei: more strength is split to this region and this strength goes to lower energies.

From the obtained results we can make a general conclusion that the presence of pairing correlations at least in one of the nucleonic subsystems causes a noticeably stronger fragmentation of both the GDR and the PDR modes comparatively the case of a normal system that was considered, for instance, in Refs. [21,22]. This effect has the two sources. First, pairing correlations lead to a diffuseness of the Fermi surface and, thus, increase the number of possible configurations of the $2q \otimes$ phonon type. The second reason for the stronger coupling

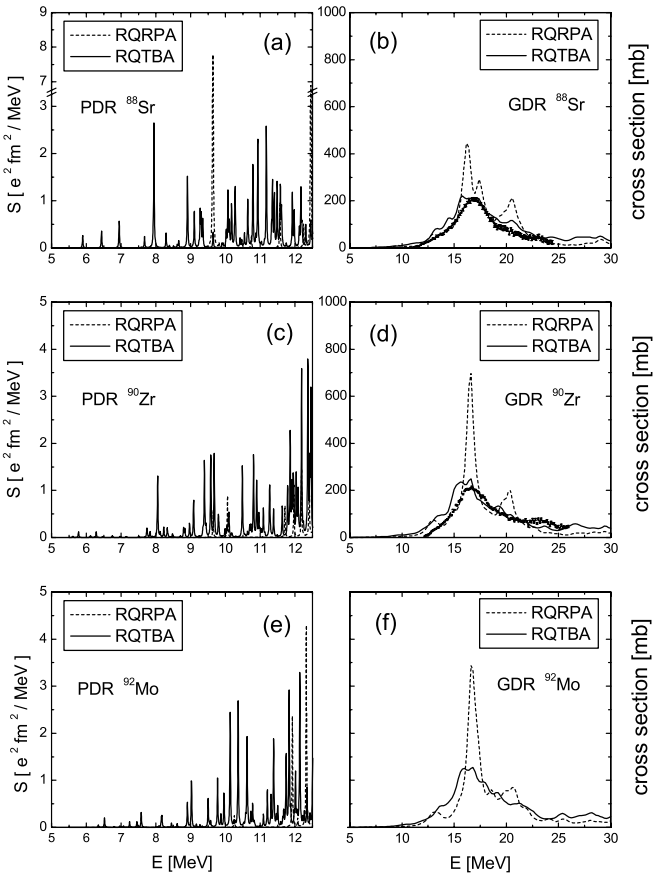

FIG. 3. The calculated dipole spectra for the $N = 50$ isotones ^{88}Sr, ^{90}Zr, ^{92}Mo. Photo absorption cross sections computed with the artificial width 400 keV (b, d, f). The low-lying portions of the corresponding spectra in terms of the strength function, calculated with 10-keV smearing (a, c, e). Calculations within the RQRPA are shown by the dashed curves, and the RQTBA by the solid curves. Experimental data are taken from Ref. [53] and are shown by black circles with bars.

effect is the considerable lowering of energies and increased transition probabilities of the lowest 2^+ states due to pairing correlations of the superfluid type. In spherical open-shell medium mass nuclei the highly collective first 2^+ states appear at energies around 1 MeV (and they are usually well reproduced in RQRPA), whereas in magic nuclei and often in nuclei near the shell closures they appear much higher, at about 3–4 MeV, and have the considerably reduced transition probabilities. This has an important physical consequence manifesting as a strong configuration mixing in the case of presence of very low-lying vibrational states. These modes admix to others, in particular, to the GDR and the PDR and the lower their energies and the higher their transition probabilities are, the stronger fragmentation they cause.

We have performed the systematic analysis of the transition densities of the RQRPA and the RQTBA states in nuclei under investigation. We have found that the $2q$ transition densities of the states in the broad low-lying energy region, originating due to the fragmentation of the RQRPA pygmy mode, have the behavior which is very similar to the behavior of the initial RQRPA state: proton and neutron components oscillate

TABLE I. Characteristics of the isovector dipole spectrum for the investigated $N = 50$ and $Z = 50$ nuclei: mean energies $\langle E \rangle$, widths Γ and energy-weighted sum rule (EWSR) values calculated with the RQRPA and with the RQRPA extended by the particle-phonon coupling (RQTBA), compared to data. The values of $\langle E \rangle$ and Γ have been obtained by a Lorentz fit of the computed strength functions within the intervals 10–22.5 MeV for $Z = 50$ and 10–25 MeV for $N = 50$ nuclei.

		$\langle E \rangle$ (MeV)	Γ (MeV)	EWSR (%)
	RQRPA	17.36	3.46	125
^{88}Sr	RQTBA	17.08	5.10	112
	RQRPA	17.03	3.15	124
^{90}Zr	RQTBA	16.72	4.77	110
	Exp. [55]	16.74	4.16	
	RQRPA	17.45	3.09	128
^{92}Mo	RQTBA	17.13	4.72	113
	Exp. [55]	16.82	4.14	
	RRPA	16.88	2.99	117
^{100}Sn	RTBA	16.39	3.43	106
	RQRPA	17.17	3.07	127
^{106}Sn	RQTBA	16.53	4.89	111
	RQRPA	16.35	3.67	126
^{114}Sn	RQTBA	15.80	5.42	106
	RQRPA	15.95	3.11	121
^{116}Sn	RQTBA	15.35	5.17	102
	Exp. [55]	15.56	5.08	
	RQRPA	15.88	3.05	121
^{120}Sn	RQTBA	15.31	5.33	104
	Exp. [55]	15.37	5.10	
	RQRPA	15.13	3.49	115
^{130}Sn	RQTBA	14.66	4.74	108
	Exp. [56]	15.9(5)	4.8(1.7)	

in phase in the nuclear interior and neutron components dominate on the surface in nuclei with noticeable neutron excess. In particular, in tin isotopes heavier than ^{114}Sn the whole energy region below 10 MeV is full of states with such behavior. Above this energy we found states with transitional behavior. Increasing further the excitation energy we observe the low-energy GDR tail with states demonstrating purely isovector underlying structure. However, the systematic numerical analysis of the transition densities is beyond the scope of the present article and will be included in the separate publication [54].

The Lorentz fit parameters for the calculated GDR in the energy intervals: (10–22.5) MeV for the tin chain and (10–25) MeV for the $N = 50$ chain are displayed in Table I and they are compared with the corresponding data of Refs. [55,56]. In our work the Lorentz fit is performed in such a way that the obtained Lorentzian has the same momenta of -2, -1, and zero orders as our microscopical strength function. This method works well if the model strength function is rather close to the Lorentz shape. From the Table I we notice that the inclusion of the particle-phonon coupling in the RQTBA calculation induces a pronounced fragmentation of the photo absorption cross sections and brings the mean energies and

TABLE II. Integral characteristics of the low-lying isovector dipole spectrum for tin isotopes: the integrated strength below 10 MeV, calculated with the RQRPA and with the RQRPA extended by the particle-phonon coupling (RQTBA), compared to the available data.

		(0–10) MeV		(0–8) MeV	
		$\sum B(E1)\uparrow$ (e^2 fm^2)	$\sum EB(E1)\uparrow$ (%)	$\sum B(E1)\uparrow$ (e^2 fm^2)	$\sum EB(E1)\uparrow$ (%)
	RRPA	0.14	0.30	0.00	0.00
^{100}Sn	RTBA	0.11	0.30	0.00	0.00
	RQRPA	0.01	0.03	0.00	0.00
^{106}Sn	RQTBA	0.14	0.30	0.02	0.04
	RQRPA	0.84	2.00	0.00	0.00
^{114}Sn	RQTBA	1.38	3.00	0.20	0.30
	RQRPA	1.78	4.00	0.00	0.00
^{116}Sn	RQTBA	1.94	4.00	0.27	0.40
	Exp. [58]			0.204(25)	
	RQRPA	3.04	6.00	0.00	0.00
^{120}Sn	RQTBA	3.08	6.00	0.62	1.00
	RQRPA	4.04	7.00	2.09	4.00
^{130}Sn	RQTBA	3.44	6.00	2.37	4.00
	Exp. [56]	3.2	7(3)		

widths of the GDR in much better agreement with the data, for all the investigated nuclei.

Because the dynamical part of the interaction amplitude in the (R)QTBA behaves as $1/\omega$ at $\omega \to \infty$ [see Eq. (54)], the first moment m_1 of the strength function is not disturbed by the coupling to phonons. This is the well-known property that has been proven for approaches of the second RPA (SRPA) type [57], including the QTBA [27]. However, additional procedures like subtraction in the self-consistent approach can change the m_1 values. Nevertheless, in Ref. [21], taking the rather broad energy region 0–30 MeV into consideration, we obtained equal values for the EWSR in the RRPA and the RTBA. To make a comparison with experimental data for the GDR, one should calculate the quantity $\sum B(EL)\uparrow$ performing the summation (integration of the energy weighted strength) within the finite energy interval investigated in the respective experimental studies of stable tin isotopes. Within such a finite energy interval the relation between the (R)QRPA and the (R)QTBA first momenta can change, and the difference depends considerably on the gross structure of the corresponding strength distributions.

In our present RQTBA calculations for $Z = 50$ and $N = 50$ nuclei the position of the GDR main peak remains almost unchanged as compared to the RQRPA. But due to the different shapes of the GDR in these two models, in particular, due to the other sharp peaks at higher energies about 18–20 MeV, appearing in the RQRPA, the RQRPA EWSR and mean energy values come out larger than those in the RQTBA calculations where we observe the very smooth GDR strength distributions close to the Lorentzian shape. In particular, the above mentioned sharp RQRPA structures around 18–20 MeV are fragmented in the RQTBA. In the nonrelativistic QTBA of Ref. [28] we dealt with the opposite situation, where the QTBA distributions came out with some additional structure on the high-energy tail that enhanced the first momentum of the strength function and, consequently, also the EWSR and the mean energy of the GDR as compared to the QRPA giving the considerably lighter high-energy tails.

The contribution of the low-lying strength to the dipole spectrum is quantified in Tables II, III. For each nucleus we have calculated the following quantities: the non-energy-weighted sum $\sum B(E1)\uparrow$, which is obtained by direct integration of the strength, and the energy-weighted quantity $\sum EB(E1)\uparrow$, which is an integral of the cross section expressed in the percentage of the classical Thomas-Reiche-Kuhn sum rule. Both quantities have been calculated with RQRPA and RQTBA to emphasize the effect of the quasiparticle-phonon coupling for the two energy intervals: (0–10) MeV and (0–8) MeV for tin isotopes and (0–S_n) and (0–8) MeV for $N = 50$ isotones. The choice of the intervals for the tin isotopes is determined by the fact that, on the one hand, in our approach we associate the pygmy modes with the dipole strength which originates from the pronounced RQRPA peaks of the isoscalar underlying structure, whose fragments in the RQTBA calculations are found in the broad energy region (4–10) MeV. On the other hand, the measurements of the low-lying strength excited in tin isotopes in the real-photon scattering experiments [58] are restricted by the energy around 8 MeV because at higher energies the sensitivity of these experiments decreases considerably. For the $N = 50$ nuclei the recent low-lying strength data of Refs. [59,60] are available up to neutron separation energies of these nuclei which are 11.11 MeV, 11.97 MeV, and 12.67 MeV for ^{88}Sr, ^{90}Zr, and ^{92}Mo, respectively, as well as the data for the lowest-energy portion of the dipole strength below 8 MeV, therefore we give the partial integral strength within these intervals.

The integral contribution of the low-energy portions calculated within the RQTBA agrees very reasonably with the available data that can be seen from Tables II and III: the inclusion of the coupling to phonons noticeably improves the description of the data. Moreover, below 8 MeV in the most of the investigated nuclei we observe that the

TABLE III. Integral characteristics of the low-lying isovector dipole spectrum below the experimental neutron thresholds S_n for the $N = 50$ nuclei: the integrated strength, calculated with the RQRPA and with the RQRPA extended by the particle-phonon coupling (RQTBA), compared to the available data.

		(0–S_n) MeV		(0–8) MeV	
		$\sum B(E1)\uparrow$ (e^2 fm^2)	$\sum EB(E1)\uparrow$ (%)	$\sum B(E1)\uparrow$ (e^2 fm^2)	$\sum EB(E1)\uparrow$ (%)
	RQRPA	0.28	0.87	0.00	0.00
^{88}Sr	RQTBA	0.66	2.06	0.13	0.32
	Exp. [59,60]			0.19(2)	
	RQRPA	0.10	0.34	0.00	0.00
^{90}Zr	RQTBA	0.86	2.83	0.07	0.17
	Exp. [59,60]			0.13(3)	
	RQRPA	0.31	1.17	0.00	0.00
^{92}Mo	RQTBA	1.28	4.42	0.03	0.06

quasiparticle-phonon coupling is the only mechanism that brings the strength to this region where the pure RQRPA has no solutions at all. We have found also general agreement of our results for ^{116,130}Sn and ^{88}Sr,^{90}Zr with the relatively recent studies of the low-lying dipole strength in Refs. [61–63] in the quasiparticle phonon model (QPM) [29], although some details of the obtained strength distributions and the behavior of the dipole transition densities are different. In the QPM based on the Skyrme interaction the model space includes up to three-phonon configurations built from a basis of QRPA states, calculated with the separable multipole-multipole residual interactions with adjustable parameters, that could be a possible source of the above mentioned differences.

Although the integral strength is described rather good within our approach, the level densities of the obtained low-lying spectra seem to be underestimated as compared to the experimental works. In the other words, in our approach the effect of fragmentation of the RQRPA excitations due to coupling to phonons is not enough. To obtain a more realistic effect, we could, obviously, use the experience of the previous calculations within the nonrelativistic models. For instance, in the Ref. [58] the calculations within the QPM model [29] with taking into account one-, two-, and three-phonon configurations lead to the better description of the PDR fine structure. Additionally, we could include at least more vibrational modes into our phonon subspace, that will not even require any modification of the model. Another way to enrich the spectrum is to take into account ground-state correlations of the singular type, according to Ref. [27].

The fragmentation of the resonances, induced by the quasiparticle-phonon coupling, is a very well known result that has been obtained long ago [64–66] (see also relatively recent calculations of electric dipole excitations in open-shell nuclei, including QPC within the framework of nonrelativistic approaches based on the Skyrme energy functional [31,67,68] as well as on the simple semiphenomenological scheme, including the single-particle continuum [28]). Actually, one finds more or less a similar level of agreement between the available experimental data and the theoretical predictions of these approaches. We notice, however, that, in general, our self-consistent relativistic approach reproduces the shapes and often the mean energies of giant dipole resonances better than the other above-mentioned approaches, that could be attributed to the more realistic form of the meson-exchange force and to the fully consistent calculation scheme.

From Figs. 2 and 3 one can see that the envelopes of the calculated GDR in ^{116,120}Sn between 10 and 22 MeV and in ^{90}Zr, ^{88}Sr between 12 and 25 MeV are rather close to the experimental cross sections. The deviations from the smooth Lorentz shape observed in experiments could be attributed to some minor drawbacks of our approach and calculation scheme: neglecting of the more complicated, than the $2q \otimes$ phonon, configurations by the time blocking, discretized continuum, restriction of the phonon subspace by the only low-lying modes, and, at last, too-simple model for the pairing force. Nevertheless, we find that the agreement with the data for the GDR cross sections in these nuclei is very good, especially taking into account the fact, that our approach is fully consistent and contains no any fit additionally to the fit of the RMF energy functional parameters NL3 that are fixed in the very beginning and used for the entire nuclear chart. Therefore, we conclude that the main mechanisms that are responsible for the damping of the GDR are taken into account correctly and consistently.

IV. OUTLOOK AND CONCLUSIONS

The RQTBA has been developed and applied for nuclear structure calculations. The physical content of this approach is the quasiparticle-vibration coupling model based on the relativistic energy density functional and the relativistic QRPA. The approach is formulated for a system with an even particle number in terms of the Bethe-Salpeter equation for the *ph* channel in the doubled space to describe a response of the system in an external field and its spectral characteristics.

The static part of the single-quasiparticle self-energy is determined by the relativistic energy functional with the parameter set NL3 based on a one-meson exchange interaction with a nonlinear self-coupling between the mesons. An independent phenomenologically parameterized term is

introduced into the relativistic energy functional to describe pairing correlations that are considered to be a nonrelativistic effect and treated in terms of Bogoliubov's quasiparticles and, in the application, within the BCS approximation. To take the QPC into account in a consistent way, we have first calculated the amplitudes of this coupling within the self-consistent RQRPA with the static interaction. Then, the calculated QPC energy-dependent self-energy was introduced into the Dirac-Hartree-BCS equation for the single-quasiparticle wave function and into the equivalent Dyson equation for a single-quasiparticle Green's function. The Bethe-Salpeter equation for the response function in the doubled space contains the energy-dependent induced interaction connected with the energy-dependent self-energy by the consistency condition. The BSE has been formulated and solved in both Dirac-Hartree-BCS and momentum-channel representations.

To solve the BSE in the quasiparticle time blocking approximation, the time-projection technique is used to block the two-quasiparticle propagation through the states that have more complicated structure than $2q \otimes$ phonon. The nuclear response is then explicitly calculated on the $2q \otimes$ phonon level by summation of infinite series of Feynman's diagrams. To avoid double counting of the QPC effects a proper subtraction of the static QPC contribution has been performed. Because the parameters of density functional for the static RMF description have been adjusted to experiment they include already essential ground-state correlations.

The RQTBA introduced in the subsection II C of this work is applied for the calculation of spectroscopic characteristics of the isovector dipole excitations in the wide energy range up to 30 MeV for spherical open-shell nuclei, in particular for the isotopes ^{100,106,114,116,120,130}Sn ($Z = 50$) and the isotones ^{88}Sr, ^{90}Zr, ^{92}Mo ($N = 50$). The QPC leads to a significant spreading width of the GDR as compared to RQRPA calculations and causes the strong fragmentation of the pygmy dipole mode and its spreading to lower energies. This is in an agreement with experimental data as well as with the results obtained within the nonrelativistic approaches.

The good agreement of our results with the experimental data obtained without any additional adjustable parameters for a large number of semimagic nuclei, confirms the universality of the RMF energy functional and the predictive power of our approach. We hope that some of the minor drawbacks of the present calculations can be overcome by using in future an improved version of the density functional both in the *ph* and in the *pp* channel.

ACKNOWLEDGMENTS

Helpful discussions with D. Vretenar are gratefully acknowledged. We are thankful to R. Schwengner for providing us with experimental results for the low-lying dipole strength in ^{88}Sr and ^{90}Zr. This work has been supported in part by the Bundesministerium für Bildung und Forschung under project 06 MT 246 and by the DFG cluster of excellence "Origin and Structure of the Universe" (www.universe-cluster.de). E.L. acknowledges the support from the Alexander von Humboldt-Stiftung. P.R. thanks for the support provided by the Ministerio de Educación y Ciencia, Spain, under the number SAB2005-0025. V.T. acknowledges financial support from the Deutsche Forschungsgemeinschaft under the grant no. 436 RUS 113/806/0-1 and from the Russian Foundation for Basic Research under the grant no. 05-02-04005-DFG_a.

APPENDIX A: DESCRIPTION OF THE GROUND STATE

In the present work we confine ourselves by the case of spherically symmetric nuclei where it is convenient to separate the dependence on the magnetic quantum number m_k: $k = \{(k), m_k\}$, where (k) is the set of remaining quantum numbers that are time reversal invariant: $-k = \{(k), -m_k\}$. In this case $(k) = \{n_k, j_k, \pi_k, \tau_k\}$ with the radial quantum number n_k, angular-momentum quantum number j_k, parity π_k, and isospin τ_k, so the Dirac spinors read:

$$\varphi_k(\mathbf{r}, t) = \begin{bmatrix} f_{(k)}(r)\, \mathcal{Y}_{l_k j_k m_k}(\vartheta, \varphi) \\ i g_{(k)}(r)\, \mathcal{Y}_{\tilde{l}_k j_k m_k}(\vartheta, \varphi) \end{bmatrix} \chi_{\tau_k}(t), \tag{A1}$$

$\mathcal{Y}_{ljm}(\vartheta, \varphi)$ is a two-component spinor

$$\mathcal{Y}_{ljm}(\vartheta, \varphi, s) = \sum_{m_s m_l} \left(\frac{1}{2} m_s l m_l | jm \right) Y_{lm_l}(\vartheta, \varphi) \chi_{m_s}(s), \tag{A2}$$

t is the coordinate for the isospin and $\chi_{\tau_k}(t)$ is a spinor in the isospin space. The orbital angular momenta l_k and $\tilde{l}_k$ of the large and small components are determined by the parity of the state k:

$$\begin{cases} l_k = j_k + \frac{1}{2}, \quad \tilde{l}_k = j_k - \frac{1}{2} & \text{for } \pi_k = (-1)^{j_k + \frac{1}{2}} \\ l_k = j_k - \frac{1}{2}, \quad \tilde{l}_k = j_k + \frac{1}{2} & \text{for } \pi_k = (-1)^{j_k - \frac{1}{2}}, \end{cases} \tag{A3}$$

$f_{(k)}(r)$ and $g_{(k)}(r)$ are radial wave functions. The phase convention for the wave function φ_{-k} is chosen so that the following relation is fulfilled:

$$\gamma^3 \gamma^1 \varphi_k^* = (-)^{l_k + j_k - m_k} \varphi_{-k}\,. \tag{A4}$$

In the literature [13] the RQRPA equations are solved for finite-range Gogny forces in the pairing channel in the canonical basis. This has the advantage, that the quasiparticle matrix elements of the QRPA equations can be calculated rather easily by multiplying the matrix elements in particle space by BCS occupation factors, but it has the disadvantage that the matrix H^{11} in quasiparticle space is no longer diagonal in the canonical basis. The quasiparticle energies $E_{k_1} + E_{k_2}$ have to be replaced by complicated matrices.

We therefore use in the following applications the RMF+BCS approximation, where the canonical basis coincides with the BCS basis. In this approximation the ground-state wave function $|\Phi_0\rangle$ is considered to be a vacuum state with respect to quasiparticles with the creation and annihilation operators $\alpha_k^\dagger, \alpha_k$ determined by the special Bogoliubov transformation:

$$\begin{pmatrix} \alpha_k \\ \alpha_{\bar{k}}^\dagger \end{pmatrix} = \begin{pmatrix} u_k & -v_k \\ v_k & u_k \end{pmatrix} \begin{pmatrix} a_k \\ a_{\bar{k}}^\dagger \end{pmatrix}, \alpha_k |\Phi_0\rangle = 0 \quad \forall k, \tag{A5}$$

where $u_k^2 + v_k^2 = 1$. Operation $\bar{k}$ transforms the state k to the time reversal state. In a spherical system we define

$$a_{\bar{k}} = (-1)^{l_k + j_k - m_k} a_{-k}, \tag{A6}$$

where the choice of the phase factors is determined by Eq. (A4).

In the RMF+BCS approximation we determine, in each step of the iteration, first the eigenfunctions φ_k of the single-particle Dirac Hamiltonian $h^{\mathcal{D}}$ of Eq. (16)

$$\int dx' h^{\mathcal{D}}(x, x')\varphi_k(x') = (m + \varepsilon_k)\varphi_k(x), \tag{A7}$$

where the coordinate $x = \{\boldsymbol{r}, \alpha, t\}$ combines the spatial coordinates $\boldsymbol{r}$ with the Dirac index $\alpha = 1 \ldots 4$ and the isospin t. Next, the Dirac spinors φ_k are used to construct the single-particle density matrix

$$\rho(x, x') = \sum_k \varphi_k(x) v_k^2 \varphi_k^\dagger(x'). \tag{A8}$$

In the basis of the functions φ_k (BCS basis) ρ as well as $h^{\mathcal{D}}$ are diagonal with the eigenvalues v_k^2 and $m + \varepsilon_k$. The pairing field Δ is in this basis close to canonical form: $\Delta_{k\bar{k}'} = \delta_{kk'}\Delta_k$. All other matrix elements vanish in the case of a monopole force with constant matrix elements and without cutoff, in other cases they are neglected in the BCS approximation. Thus, in this basis, the Hartree-Bogoliubov matrix (14) is reduced to a set of 2×2 matrices, which can be diagonalized analytically. One finds as eigenvalues the quasiparticle energies

$$E_k = \sqrt{(\varepsilon_k - \lambda_{\tau_k})^2 + \Delta_k^2} \tag{A9}$$

and as eigenfunctions the occupation amplitudes u_k and v_k with

$$v_k^2 = \frac{1}{2}\left(1 - \frac{\varepsilon_k - \lambda_{\tau_k}}{E_k}\right) \tag{A10}$$

and $u_k = \sqrt{1 - v_k^2}$. The pairing gaps Δ_k are obtained by the solution of the gap equation

$$\Delta_k = -\frac{1}{2}\sum_{k'} V^{pp}_{k\bar{k},k'\bar{k}'} \frac{\Delta_{k'}}{2E_{k'}} \tag{A11}$$

in each step of the iteration and the chemical potential λ_{τ_k} is fixed via particle number conservation:

$$\sum_k v_k^2 = N(\text{or } Z) \quad \text{for neutrons (or protons).} \tag{A12}$$

After the solution of the BCS equations (A11)–(A12) the density (A8) is calculated and used for the solution of the Klein-Gordon equations (22) determining the RMF potentials for the Dirac-Hartree Hamiltonian in Eq. (A7) in the next step of the iteration. In the RMF+BCS approximation the eight components of the quasiparticle eight-component Dirac spinor $|\psi_k^\eta\rangle$ are simply expressed through the usual four-component spinor wave functions φ_k:

$$\begin{aligned} U_k(x) &= u_k\varphi_k(x) \\ V_k(x) &= (-1)^{l_k + j_k + m_k} v_k \varphi^*_{-k}(x), \end{aligned} \tag{A13}$$

and we have chosen $u_k, v_k > 0\,\forall k$. This simplifies the calculation of the RQRPA matrix elements in the next section considerably. We only have to calculate the matrix elements in particle space using the wave functions φ_k and multiply them with the corresponding BCS occupation factors in Eqs. (B6) and (B7).

In the present applications of our approach we use a monopole pairing force with constant matrix elements and a soft pairing window. Details are given in Appendix B.

APPENDIX B: SOLUTION OF THE RQRPA EQUATIONS AND CALCULATION OF THE PHONON VERTICES

The RQRPA equations are derived as the small amplitude limit of the time-dependent Dirac-Hartree-Bogoliubov equations for the generalized density matrix $\mathcal{R}$ [13]. For general pairing forces, as, for instance, for the finite range Gogny force in the pairing channel [69], they can be solved in the canonical basis [70] of the RHB equations, where the full Hartree-Bogoliubov ground-state wave function has BCS form. In the RMF+BCS case they are solved in the Dirac-Hartree-BCS basis (A13) described above. In spherical systems we can use angular-momentum coupling of the two-quasiparticle states and the reduced form of the RQRPA equation for angular momentum J_μ is:

$$\left(\eta\Omega_\mu - E_{k_1} - E_{k_2}\right)\mathcal{R}^\eta_{\mu(k_1k_2)} = \sum_{\eta'} \sum_{(k_4) \leqslant (k_3)} \tilde{V}^{J_\mu,\eta\eta'}_{(k_1k_4,k_2k_3)} \mathcal{R}^{\eta'}_{\mu(k_3k_4)}, \tag{B1}$$

where the index μ characterizes the various solutions of the RQRPA equation, in particular their angular momentum J_μ. The notation (k_1k_2) indicates that the two quasiparticles with the indices k_1 and k_2 are coupled to angular momentum J_μ. The $\eta\eta'$ components of the static residual interaction in the ph channel read:

$$\begin{aligned} &\tilde{V}^{J,\eta\eta'}_{(k_1k_4,k_2k_3)} \\ &\quad = \sum_{S=0,1} [\delta_{\eta,1} + (-1)^S\delta_{\eta,-1}][\delta_{\eta',1} + (-1)^S\delta_{\eta',-1}] \\ &\qquad \times \left[\eta^S_{(k_1k_2)}\eta^S_{(k_3k_4)}\tilde{v}^{(ph)JS}_{(k_1k_4,k_2k_3)} + \xi^S_{(k_1k_2)}\xi^S_{(k_3k_4)}\tilde{v}^{(pp)J}_{(k_1k_2,k_3k_4)}\right], \end{aligned} \tag{B2}$$

where $\tilde{v}^{(ph)JS}_{(k_1k_4,k_2k_3)}$ and $\tilde{v}^{(pp)J}_{(k_1k_2,k_3k_4)}$ are the reduced matrix elements of the ph and pp interaction. We assume that the pp components do not depend on the total spin, and the ph components carry spin $S = 0, 1$. The ph components $\tilde{v}^{(ph)JS}_{(k_1k_4,k_2k_3)}$ describe the one-boson exchange (OBE) interaction and could be expressed as follows:

$$\begin{aligned} \tilde{v}^{(ph)JS}_{(k_1k_4,k_2k_3)} = \pm\frac{(4\pi)^2}{2J+1}\sum_{m\in S}\sum_L \int_0^\infty \frac{q^2q'^2dqdq'}{(2\pi)^6} \\ \times \langle(k_1)\|j_L(qr)[\beta\Gamma_{mS}Y_L]^J\|(k_2)\rangle \\ \times D^S_m(q,q')\langle(k_3)\|j_L(q'r)[\beta\Gamma_{mS}Y_L]^J\|(k_4)\rangle, \end{aligned} \tag{B3}$$

where in the first sum ($m \in S$) the index m runs over the various meson fields carrying spin S. The index S in Γ_{mS} denotes the spin of the Pauli matrix entering the vertices Γ_m in Eq. (7). This implies in particular that $S = 0$ for the scalar and timelike parts of the vector mesons and that $S = 1$ for the spacelike parts of the vector mesons (current-current interactions).

Representing the q integral in Eq. (B3) by a discrete sum over mesh points, the matrix elements (B3) are a sum of separable terms. The nonlocal meson propagator is a solution of the integral equation:

$$\boldsymbol{q}^2 D_m^S(\boldsymbol{q},\boldsymbol{q}') + \int \frac{d^3q''}{(2\pi)^3} M_m^S(\boldsymbol{q}-\boldsymbol{q}'') D_m^S(\boldsymbol{q}'',\boldsymbol{q}') = (2\pi)^3\delta(\boldsymbol{q}-\boldsymbol{q}'), \tag{B4}$$

where $M_m^S(\boldsymbol{q})$ is the Fourier transform of $U''[\phi_m^S(\boldsymbol{r})]$ determined by Eqs. (8), (9):

$$M_m^S(\boldsymbol{q}) = \int d^3r e^{-i\boldsymbol{q}\boldsymbol{r}} U''\big[\phi_m^S(\boldsymbol{r})\big]. \tag{B5}$$

The quantities $\eta^S_{(k_1k_2)}$, $\xi^S_{(k_1k_2)}$ in the Eq. (B2) are the conventional factors [70] which are the following linear combinations of the occupation numbers:

$$\eta^S_{(k_1k_2)} = \frac{1}{\sqrt{1+\delta_{(k_1k_2)}}}\big[u_{k_1}v_{k_2} + (-1)^S v_{k_1}u_{k_2}\big] \tag{B6}$$

$$\xi^S_{(k_1k_2)} = \frac{1}{\sqrt{1+\delta_{(k_1k_2)}}}\big[u_{k_1}u_{k_2} - (-1)^S v_{k_1}v_{k_2}\big], \tag{B7}$$

arising due to symmetrization in the integral part of the Eq. (B1), which enables one to take each $2q$ pair into account only once because of the symmetry properties of the reduced matrix elements $\tilde{v}^{(ph)JS}_{(k_1k_4,k_2k_3)}$ and $\tilde{v}^{(pp)J}_{(k_1k_2,k_3k_4)}$. For the interaction $\tilde{v}^{(pp)}$ in the pp channel we use a simple monopole-monopole ansatz with the so-called smooth window [71]:

$$\tilde{v}^{(pp)J}_{(k_1k_2,k_3k_4)} = -\frac{G}{2}\,\delta_{J0}\delta_{(k_1k_2)}\delta_{(k_3k_4)}\sqrt{\frac{2j_{k_1}+1}{1+e^{(\varepsilon_{k_1}-w)/d}}} \times\sqrt{\frac{2j_{k_3}+1}{1+e^{(\varepsilon_{k_3}-w)/d}}}, \tag{B8}$$

where w is the value of the pairing window and d is its diffuseness.

The RQRPA transition densities $\mathcal{R}^{\eta}_{\mu(k_1k_2)}$ calculated from the Eq. (B1) determine in particular the components of the amplitudes $\gamma^{\eta}_{\mu(k_1k_2)}$ that couple the phonon with the quasiparticle states $|\psi^{\eta_1}_{k_1}\rangle$ and $|\psi^{\eta_2}_{k_2}\rangle$ having $\eta_1=\eta_2=\eta$, i.e., lying on the same side with respect to the Fermi level

$$\begin{aligned}\gamma^{\eta}_{\mu(k_1k_2)} = {}& \sqrt{1+\delta_{(k_1k_2)}}\sum_{\eta'}\sum_{(k_4)\le(k_3)} \times\sum_{S=0,1}[\delta_{\eta,1}-(-1)^S\delta_{\eta,-1}][\delta_{\eta',1}+(-1)^S\delta_{\eta',-1}] \\ &\times\big[\xi^S_{(k_1k_2)}\eta^S_{(k_3k_4)}\tilde{v}^{(ph)J_\mu S}_{(k_1k_4,k_2k_3)} - \eta^S_{(k_1k_2)}\xi^S_{(k_3k_4)}\tilde{v}^{(pp)J_\mu}_{(k_1k_2,k_3k_4)}\big]\mathcal{R}^{\eta'}_{\mu(k_3k_4)}.\end{aligned} \tag{B9}$$

APPENDIX C: THE RQTBA CORRELATED PROPAGATOR AND THE STRENGTH FUNCTION

In solving Eq. (47) for the response function, we use our previous experience with calculations for nuclei with closed shells [21,22]. Again, we formulate and solve this equation both in the $2q$ basis of Dirac-Hartree-BCS quasiparticle pairs and in the momemtum-channel space. In Dirac-Hartree-BCS space its dimension is the number of $2q$ pairs that satisfy the selection rules for the given multipolarity. In relativistic nuclear calculations it is always important to take into account the contribution of the Dirac sea. This can be done, as it is done traditionally, explicitly, or statically by the renormalization of the static interaction, as it is proposed in Ref. [50]. Nevertheless, for systems with pairing correlations the total number of $2q$ pairs entering Eq. (47) increases considerably not only with the nuclear mass number but also with the pairing window. As it was investigated in a series of RRPA calculations [12,72], the completeness of the ph (αh) basis is very important for calculations of giant resonance characteristics as well as for current conservation and a proper treatment of symmetries, in particular, the dipole spurious state originating from the violation of translation symmetry on the mean-field level. However, the use of a large basis requires a considerable numerical effort and, therefore, it is reasonable to solve the Eq. (47) in a different more appropriate representation.

Our choice is determined by the following properties of the static effective interaction $\tilde{V}$. Its ph component is based on the exchange of mesons and explicitly contains only direct terms and no exchange terms, therefore it can be written as a sum of separable interactions (B3), and in the present work its pp component is also chosen in the separable form (B8) for convenience.

As in Refs. [21,22], we solve the response equation for a fixed value of the energy variable ω in two steps. First, we calculate the correlated propagator $R^e(\omega)$ that describes the propagation under the influence of the interaction $\Phi(\omega)$ in the time blocking approximation without GSC caused by the phonon coupling:

$$\begin{aligned}R^{(e)J,\eta}_{(k_1k_4,k_2k_3)}(\omega) = {}& \tilde{R}^{(s)J,\eta}_{(k_1k_4,k_2k_3)}(\omega) \\ &+ \tilde{R}^{(0)\eta}_{(k_1k_2)}(\omega)\sum_{(k_6\le k_5)}\big[\Phi^{(s)J,\eta}_{(k_1k_6,k_2k_5)}(\omega) \\ &- \Phi^{(s)J,\eta}_{(k_1k_6,k_2k_5)}(0)\big]R^{(e)J,\eta}_{(k_5k_4,k_6k_3)}(\omega),\end{aligned} \tag{C1}$$

where the symmetrized matrix elements of the mean-field propagator $\tilde{R}^{(s)}$ and the two quasiparticles-phonon coupling amplitude $\Phi^{(s)}$ read:

$$\begin{aligned}\tilde{R}^{(s)J,\eta}_{(k_1k_4,k_2k_3)}(\omega) = {}& \tilde{R}^{(0)\eta}_{(k_1k_2)}(\omega)\big[\delta_{(k_1k_3)}\delta_{(k_2k_4)} \\ &+ (-)^{J+l_1-l_2+j_1-j_2}\delta_{(k_1k_4)}\delta_{(k_2k_3)}\big],\end{aligned} \tag{C2}$$

$$\begin{aligned}\Phi^{(s)J,\eta}_{(k_1k_4,k_2k_3)}(\omega) = {}& \frac{1}{1+\delta_{(k_3k_4)}}\big[\Phi^{J,\eta}_{(k_1k_4,k_2k_3)}(\omega) \\ &+ (-)^{J+l_1-l_2+j_1-j_2}\Phi^{J,\eta}_{(k_2k_4,k_1k_3)}(\omega)\big],\end{aligned} \tag{C3}$$

which means that we take into account two kinds of components: one kind with only forward ($\eta=1$) $2q$ propagators of the ph type ($\eta_1=-\eta_2$) and another one with only backward

propagators ($\eta = -1$), but do not include mixed ones. In the conventional terminology it means that we neglect ground-state correlations caused by the quasiparticle-phonon coupling. The reduced matrix elements of the quasiparticle-phonon coupling amplitude $\Phi^{J,\eta}_{(k_1k_4,k_2k_3)}(\omega)$ read:

$$\Phi^{J,\eta}_{(k_1k_4,k_2k_3)}(\omega) = \sum_\mu \Bigg(\frac{\delta_{(k_1k_3)}\delta_{\varkappa_{k_4}\varkappa_{k_2}}}{2j_{k_2}+1} \sum_{(k_6)} \frac{\gamma^{-\eta}_{\mu(k_6k_2)}\gamma^{-\eta*}_{\mu(k_6k_4)}}{\eta\omega - E_{k_1} - E_{k_6} - \Omega_\mu} + \frac{\delta_{(k_2k_4)}\delta_{\varkappa_{k_3}\varkappa_{k_1}}}{2j_{k_1}+1} \sum_{(k_5)} \frac{\gamma^{\eta}_{\mu(k_1k_5)}\gamma^{\eta*}_{\mu(k_3k_5)}}{\eta\omega - E_{k_5} - E_{k_2} - \Omega_\mu} + (-1)^{J+J_\mu} \begin{Bmatrix} j_{k_1} & j_{k_2} & J \\ j_{k_4} & j_{k_3} & J_\mu \end{Bmatrix} \times \Bigg[\frac{(-1)^{j_{k_3}-j_{k_2}}\gamma^{\eta}_{\mu(k_1k_3)}\gamma^{-\eta*}_{\mu(k_2k_4)}}{\eta\omega - E_{k_3} - E_{k_2} - \Omega_\mu} + \frac{(-1)^{j_{k_1}-j_{k_4}}\gamma^{\eta*}_{\mu(k_3k_1)}\gamma^{-\eta}_{\mu(k_4k_2)}}{\eta\omega - E_{k_1} - E_{k_4} - \Omega_\mu} \Bigg] \Bigg), \tag{C4}$$

where $\varkappa_k$ denotes the relativistic quantum number set: $\varkappa_k = (2j_k+1)(l_k - j_k)$. The reduced matrix elements of the particle-phonon coupling amplitude $\gamma^{\eta}_{\mu(k_1k_2)}$ are calculated from the Eq. (B9). The index $\mu = \{J_\mu, n_\mu\}$ denotes the set of phonon quantum numbers that are its angular momentum J_μ and the number of the solution n_μ of the Eq. (B1). The quantity Ω_μ is the corresponding energy. The fact that the right-hand side of Eq. (C4) depends only on the same η values as the left-hand side and contains no mixing of different η values implies that no GSC are contained in the intermediate $2q \otimes$ phonon propagators.

The Eq. (C1) is too expensive numerically to be solved in the full Dirac-Hartree-BCS basis. However, due to the pole structure of the Φ amplitude it is naturally to suggest that quasiparticle-phonon coupling effects are not important quantitatively far from the Fermi surface. In the present work, for numerical calculations an energy window $E_{\rm win}$ was implemented around the Fermi surface with respect to pure two-quasiparticle energies E_{2q} so the summation in the Eq. (C1) is performed only among the $2q$ pairs with $E_{2q} \leqslant E_{\rm win}$. Consequently, the correlated propagator differs from the mean-field propagator only within this window. This approximation has been checked in the Ref. [21] in the calculations for nuclei with closed shells by direct calculations with different values of this energy window, and it has been found that this window should include just the investigated energy region. Beyond the energy window we do not obtain additional poles caused by $2q \otimes$ phonon configurations but only the renormalized QRPA spectrum. It is important to emphasize that many $2q$ and αq configurations outside of the window are taken into account on the RQRPA level that is necessary to obtain the reasonable centroid positions of giant resonances as well as to find the dipole spurious state close to zero energy. By its physical meaning, the Eq. (C1) contains all effects of the quasiparticle-phonon coupling and all the singularities of the integral part of the initial BSE.

In the second step, we have to solve the remaining equation for the full response function $R(\omega)$:

$$R^{J,\eta\eta'}_{(k_1k_4,k_2k_3)}(\omega) = R^{(e)J,\eta}_{(k_1k_4,k_2k_3)}(\omega)\delta_{\eta\eta'} + \sum_{(k_6 \leqslant k_5)} \sum_{(k_8 \leqslant k_7)\eta''} R^{(e)J,\eta}_{(k_1k_6,k_2k_5)}(\omega)\tilde{V}^{J,\eta\eta''}_{(k_5k_8,k_7k_6)}R^{J,\eta''\eta'}_{(k_7k_4,k_8k_3)}(\omega). \tag{C5}$$

In contrast to the Eq. (C1), this equation contains only the static effective interaction $\tilde{V}$ from the Eq. (B2).

Because both the one-boson exchange interaction and the pairing interaction are separable in momentum space, we can use this advantage and formulate the response equation in the momentum-channel representation. Let us introduce the following generalized channel index $c_\chi = \{q, m, L, S\}$ for $\chi = (ph)$ and $c_\chi = S$ for $\chi = (pp)$. For $\chi = (ph)$ it includes the momentum q transferred in the exchange process of the corresponding meson labeled by the index m. The index χ distinguishes ph- and pp-channel components of the static interaction, L is the angular momentum, and the index $S = 0, 1$ has its usual meaning of the total spin carried through the certain channel. In this way, we apply the following ansatz for the η components of the static effective interaction $\tilde{V}$

$$\tilde{V}^{(J)\eta\eta'}_{(k_1k_4,k_2k_3)} = \sum_{cc'} Q^{(c)J,\eta}_{(k_1k_2)} d_{cc'} Q^{(c')J,\eta'*}_{(k_3k_4)}, \tag{C6}$$

where we omit the index χ for simplicity. For the channels with $\chi = (ph)$:

$$Q^{(c)J,\eta}_{(k_1k_2)} = \frac{\delta_{\eta,1} + (-1)^S\delta_{\eta,-1}}{\sqrt{1+\delta_{(k_1k_2)}}} \times \eta^S_{(k_1k_2)}\langle (k_1)\| j_L(qr)[\beta\Gamma_{mS}Y_L]^J \|(k_2)\rangle \tag{C7}$$

$$d_{cc'} = \pm\frac{1}{2J+1}\frac{D^S_m(q,q')}{(2\pi)^6}\delta_{LL'}\delta_{SS'}\delta_{mm'} \tag{C8}$$

and the summation over c, c' implies integration over d^3q, d^3q'. For the channels with $\chi = (pp)$ we have:

$$Q^{(c)J,\eta}_{(k_1k_2)} = \delta_{J0}\delta_{(k_1k_2)}\frac{\delta_{\eta,1} + (-1)^S\delta_{\eta,-1}}{\sqrt{1+\delta_{(k_1k_2)}}}\xi^S_{(k_1k_2)}\sqrt{\frac{2j_{k_1}+1}{1+e^{(\varepsilon_{k_1}-w)/d}}} \tag{C9}$$

$$d_{cc'} = -\frac{G}{2}\delta_{cc'}. \tag{C10}$$

Then, we can use the well-known techniques of the response formalism with separable interactions (see, for instance, Ref. [70]). We define the exact response function and the correlated propagator in the generalized momentum-channel space as follows:

$$R^J_{cc'}(\omega) = \sum_{(k_2 \leqslant k_1)\eta} \sum_{(k_4 \leqslant k_3)\eta'} Q^{(c)J,\eta*}_{(k_1k_2)} R^{J,\eta\eta'}_{(k_1k_4,k_2k_3)}(\omega) Q^{(c')J,\eta'}_{(k_3k_4)} R^{(e)J}_{cc'}(\omega) \tag{C11}$$

$$= \sum_{(k_2 \leqslant k_1)} \sum_{(k_4 \leqslant k_3)\eta} Q^{(c)J,\eta*}_{(k_1k_2)} R^{(e)J,\eta}_{(k_1k_4,k_2k_3)}(\omega) Q^{(c')J,\eta}_{(k_3k_4)}. \tag{C12}$$

In this representation Eq. (C5) reads:

$$R_{cc'} = R^e_{cc'} + (R^e d R)_{cc'}. \tag{C13}$$

This equation is solved by matrix inversion

$$R = \left(1 - R^e d\right)^{-1} R^e. \tag{C14}$$

To compute the nuclear response in the certain external field, we need a convolution of the exact response function with the external field operator P that can be suggested as an additional channel $c = p$, $p = \{z, \chi\}$, where the index z contains possible additional dependences of the external field that we do not concretize here:

$$P^{(p)J,\eta}_{(k_1k_2)} = \sum_{LS} \frac{\delta_{\eta,1} + (-1)^S \delta_{\eta,-1}}{\sqrt{1+\delta_{(k_1k_2)}}} \eta^S_{(k_1k_2)} \langle (k_1) \| \; P^{(p)J}_{LS} \| \; (k_2) \rangle. \tag{C15}$$

Making use of this definition, we can determine the polarizability as:

$$\Pi^J(\omega) = R^J_{pp}(\omega) = R^{(e)J}_{pp}(\omega) + \sum_{cc'} R^{(e)J}_{pc}(\omega) d_{cc'} R^J_{c'p}(\omega), \tag{C16}$$

where the quantities $R^{(e)J}_{pc}(\omega)$, $R^{(e)J}_{pp}(\omega)$ can be found as follows:

$$R^{(e)J}_{pc}(\omega) = \sum_{(k_2 \leqslant k_1)} \sum_{(k_4 \leqslant k_3)\eta} P^{(p)J,\eta *}_{(k_1k_2)} R^{(e)J,\eta}_{(k_1k_4,k_2k_3)}(\omega) Q^{(c)J,\eta}_{(k_3k_4)} \tag{C17}$$

$$R^{(e)J}_{pp}(\omega) = \sum_{(k_2 \leqslant k_1)} \sum_{(k_4 \leqslant k_3)\eta} P^{(p)J,\eta *}_{(k_1k_2)} R^{(e)J,\eta}_{(k_1k_4,k_2k_3)}(\omega) P^{(p)J,\eta}_{(k_3k_4)},$$

and the quantity $R^J_{cp}(\omega)$, which has a meaning of the density matrix variation in the external field P, obeys the equation:

$$R^J_{cp}(\omega) = R^{(e)J}_{cp}(\omega) + \sum_{c'c''} R^{(e)J}_{cc'}(\omega) d_{c'c''} R^J_{c''p}(\omega). \tag{C18}$$

To describe the observed spectrum of the excited nucleus in a weak external field P, as for instance a dipole field, one needs to calculate the strength function:

$$S^J(E) = -\frac{1}{\pi} \lim_{\Delta \to +0} Im \Pi^J(E + i\Delta), \tag{C19}$$

expressed through the polarizability $\Pi^J(\omega)$ defined by Eq. (C16).

Obviously, the dimension of vectors and matrices entering Eq. (C18) is determined by the number of mesh points in q space and the number of m, L, S channels. In particular, it does not depend considerably on the total dimension of $2q$ and αq subspaces and on the mass number of the nucleus. As we have realized in the calculations of Refs. [21,22], the advantage of the momentum-channel representation appears at some medium values of the nuclear mass number, where the total dimension of ph and αh subspaces, which is exactly the dimension of arrays in the Eq. (50) written in the coupled form, become comparable with the dimension of matrices entering Eq. (C18). In the present approach, due to the pairing correlations, this mass region shifts toward lower masses. The solution in the momentum-channel space is even more helpful when we include pairing correlations, because the number of states within the pairing window increases by more than a factor 2 as compared to the case without pairing. For heavy nuclei the dimension of the two-quasiparticle DHBCS basis increases considerably and, therefore, for heavy nuclei the solution of the response equations in momentum space is recommendable.

Notice, that the pairing correlations cause also an additional numerical effort in Eq. (C1). It is solved within the subspace of $2q$ configurations confined by the $E_{\rm win}$ that, in the realistic calculations, surrounds the pairing window and, therefore, contains considerably more configurations as compared to the case of no pairing.

[1] P. Ring, Prog. Part. Nucl. Phys. **37**, 193 (1996).
[2] D. Vretenar, A. V. Afanasjev, G. A. Lalazissis, and P. Ring, Phys. Rep. **409**, 101 (2005).
[3] Y. K. Gambhir, P. Ring, and A. Thimet, Ann. Phys. (NY) **198**, 132 (1990).
[4] G. A. Lalazissis, D. Vretenar, and P. Ring, Eur. Phys. J. A **22**, 37 (2004).
[5] G. A. Lalazissis, M. M. Sharma, P. Ring, and Y. K. Gambhir, Nucl. Phys. **A608**, 202 (1996).
[6] T. Bürvenich, M. Bender, J. A. Maruhn, and P.-G. Reinhard, Phys. Rev. C **69**, 014307 (2004).
[7] J. Meng and P. Ring, Phys. Rev. Lett. **77**, 3963 (1996).
[8] G. A. Lalazissis, D. Vretenar, and P. Ring, Phys. Rev. C **69**, 017301 (2004).
[9] G. A. Lalazissis, D. Vretenar, and P. Ring, Nucl. Phys. **A650**, 133 (1999).
[10] W. Koepf and P. Ring, Nucl. Phys. **A493**, 61 (1989).
[11] A. V. Afanasjev, P. Ring, and J. König, Nucl. Phys. **A676**, 196 (2000).
[12] P. Ring, Z.-Y. Ma, N. Van Giai, D. Vretenar, A. Wandelt, and L.-G. Cao, Nucl. Phys. **A694**, 249 (2001).
[13] N. Paar, P. Ring, T. Nikšić, and D. Vretenar, Phys. Rev. C **67**, 034312 (2003).
[14] A. Ansari, Phys. Lett. **B623**, 37 (2005).
[15] A. Ansari and P. Ring, Phys. Rev. C **74**, 054313 (2006).
[16] N. Paar, T. Nikšić, D. Vretenar, and P. Ring, Phys. Rev. C **69**, 054303 (2004).
[17] D. Vretenar, T. Nikšić, and P. Ring, Phys. Rev. C **65**, 024321 (2002).
[18] E. Litvinova and P. Ring, Phys. Rev. C **73**, 044328 (2006).
[19] T. Nikšić, D. Vretenar, and P. Ring, Phys. Rev. C **73**, 034308 (2006).
[20] T. Nikšić, D. Vretenar, and P. Ring, Phys. Rev. C **74**, 064309 (2006).
[21] E. Litvinova, P. Ring, and V. I. Tselyaev, Phys. Rev. C **75**, 064308 (2007).
[22] E. Litvinova, P. Ring, and D. Vretenar, Phys. Lett. **B647**, 111 (2007).
[23] V. I. Tselyaev, Yad. Fiz. **50**, 1252 (1989).
[24] V. I. Tselyaev, Sov. J. Nucl. Phys. **50**, 780 (1989).
[25] S. P. Kamerdzhiev, G. Y. Tertychny, and V. I. Tselyaev, Phys. Part. Nuclei **28**, 134 (1997).
[26] S. P. Kamerdzhiev, J. Speth, and G. Y. Tertychny, Phys. Rep. **393**, 1 (2004).
[27] V. I. Tselyaev, Phys. Rev. C **75**, 024306 (2007).

[28] E. V. Litvinova and V. I. Tselyaev, Phys. Rev. C **75**, 054318 (2007).
[29] V. G. Soloviev, *Theory of Atomic Nuclei: Quasiparticles and Phonons* (Institute of Physics, Bristol and Philadelphia, 1992), textbook on QPM.
[30] C. A. Bertulani and V. Y. Ponomarev, Phys. Rep. **321**, 139 (1999).
[31] G. Colò and P. F. Bortignon, Nucl. Phys. **A696**, 427 (2001).
[32] A. Bohr and B. Mottelson, *Nuclear Structure* (Benjamin, Reading, MA, 1975), Vol. II.
[33] J. G. Valatin, Phys. Rev. **122**, 1012 (1961).
[34] H. Kucharek, PhD thesis, Technical University of Munich (unpublished, 1989).
[35] H. Kucharek and P. Ring, Z. Phys. A **339**, 23 (1991).
[36] M. Serra, A. Rummel, and P. Ring, Phys. Rev. C **65**, 014304 (2001).
[37] M. Serra and P. Ring, Phys. Rev. C **65**, 064324 (2002).
[38] L. P. Gor'kov, Sov. Phys. JETP **34**, 505 (1958).
[39] W. Brenig and H. Wagner, Z. Phys. **173**, 484 (1963).
[40] J. D. Walecka, Ann. Phys. (NY) **83**, 491 (1974).
[41] B. D. Serot and J. D. Walecka, Adv. Nucl. Phys. **16**, 1 (1986).
[42] J. Boguta and A. R. Bodmer, Nucl. Phys. **A292**, 413 (1977).
[43] S. A. Fayans, S. V. Tolokonnikov, E. L. Trykov, and D. Zawischa, Nucl. Phys. **A676**, 49 (2000).
[44] G. F. Bertsch and H. Esbensen, Ann. Phys. (NY) **209**, 327 (1991).
[45] K. Capelle and E. K. U. Gross, Phys. Rev. B **59**, 7140 (1999).
[46] A. A. Abrikosov, L. P. Gor'kov, and I. E. Dzyaloshincki, *Methods of Quantum Field Theory in Statistical Physics* (Prentice Hall, Engelwood Cliffs, NJ, 1963).
[47] J. F. Dawson and R. J. Furnstahl, Phys. Rev. C **42**, 2009 (1990).
[48] Z.-Y. Ma, N. Van Giai, H. Toki, and M. L'Huillier, Phys. Rev. C **55**, 2385 (1997).
[49] D. Pena Arteaga and P. Ring, Phys. Rev. C **77**, 034317 (2008).
[50] V. I. Tselyaev, E. Litvinova, D. Pena, and P. Ring (to be published, 2008).
[51] G. A. Lalazissis, J. König, and P. Ring, Phys. Rev. C **55**, 540 (1997).
[52] P. Papakonstantinou, Eur. Phys. Lett. **78**, 12001 (2007).
[53] Experimental Nuclear Reaction Data, http://www-nds.iaea.or.at/exfor/exfor00.htm.
[54] E. Litvinova, P. Ring, V. Tselyaev, and K. Langanke, to be published (2008).
[55] Reference Input Parameter Library, Version 2, http://www-nds.iaea.org/RIPL-2/.
[56] P. Adrich *et al*., Phys. Rev. Lett. **95**, 132501 (2005).
[57] S. Adachi and E. Lipparini, Nucl. Phys. **A489**, 445 (1988).
[58] K. Govaert *et al*., Phys. Rev. C **57**, 2229 (1998).
[59] R. Schwengner, G. Rusev, N. Benouaret *et al*., Phys. Rev. C **76**, 034321 (2007).
[60] R. Schwengner and A. Wagner (private communication).
[61] N. Tsoneva, H. Lenske, and C. Stoyanov, Nucl. Phys. **A731**, 273 (2004).
[62] N. Tsoneva and H. Lenske, J. Phys. G **35**, 014047 (2008).
[63] N. Tsoneva and H. Lenske, Phys. Rev. C **77**, 024321 (2008).
[64] V. G. Soloviev, C. Stoyanov, and A. I. Vdovin, Nucl. Phys. **A288**, 376 (1977).
[65] G. F. Bertsch, P. F. Bortignon, R. A. Broglia, and C. H. Dasso, Phys. Lett. **B80**, 161 (1979).
[66] P. F. Bortignon and R. A. Broglia, Nucl. Phys. **A371**, 405 (1981).
[67] D. Sarchi, P. F. Bortignon, and G. Colo, Phys. Lett. **B601**, 27 (2004).
[68] A. Avdeenkov, F. Grümmer, S. Kamerdzhiev, S. Krewald, N. Lyutorovich, and J. Speth, Phys. Lett. **B653**, 196 (2007).
[69] T. Gonzales-Llarena, J. L. Egido, G. A. Lalazissis, and P. Ring, Phys. Lett. **B379**, 13 (1996).
[70] P. Ring and P. Schuck, *The Nuclear Many-Body Problem* (Springer, Heidelberg, 1980).
[71] P. Bonche, H. Flocard, P.-H. Heenen, S. J. Krieger, and M. S. Weiss, Nucl. Phys. **A443**, 39 (1985).
[72] Z.-Y. Ma, A. Wandelt, N. Van Giai, D. Vretenar, P. Ring, and L.-G. Cao, Nucl. Phys. **A703**, 222 (2002).